Journal of Molecular Liquids 294 (2019) 111560

Contents lists available at ScienceDirect

Journal of Molecular Liquids

journal homepage: www.elsevier.com/locate/molliq

Amphiphilic silicone-bridged bis-triazoles as effective, selective metal ligands and biologically active agents in lipophilic environment

Georgiana-Oana Turcan-Trofin [a], Mirela-Fernanda Zaltariov [a], Gheorghe Roman [a], Sergiu Shova [a], Nicoleta Vornicu [b], Mihaela Balan-Porcarasu [a], Dragos Lucian Isac [a], Andrei Neamtu [c,a], Maria Cazacu [a,*]

[a] Department of Inorganic Polymers, "Petru Poni" Institute of Macromolecular Chemistry, Aleea Gr. Ghica Voda 41 A, Iasi 700487, Romania
[b] Metropolitan Center of Research T.A.B.O.R, The Metropolitanate of Moldavia and Bukovina, Iasi, Romania
[c] Regional Institute of Oncology (IRO), TRANSCEND Research Center, str. General Henry Mathias Berthlot nr. 2-4, Iasi, Romania

ARTICLE INFO

Article history:
Received 24 April 2019
Received in revised form 6 July 2019
Accepted 10 August 2019
Available online 12 August 2019

Keywords:
Amphiphile ligands
Triazoles on silicone substrate
Chemosensors
Biologically active ligands
Self-assembly

ABSTRACT

Pairs of different substituted 3-mercapto-1,2,4-triazole units are coupled, through thioether bridges, to organic-inorganic substrates consisting in short hydrophobic silicone segment. A library of six compounds are isolated as crystalline solids and structurally characterized by X-ray single crystal diffraction, elemental, spectral and thermal analysis. The flexibility of the silicone spacer makes the small molecular compounds exhibit glass transition in the negative domain. The metal binding capacity is evaluated by quantum mechanics calculations, the results being in line with experimental data obtained by UV–vis spectroscopy titration. The results indicate that the prepared compounds can act as ligands for metal ions with high selectivity for Cu^{2+}, an element of interest in biological processes, forming 1:1 stable mononuclear complexes with an association constant up to 8.87 $\times 10^3$ M^{-1}. The presence of the highly hydrophobic silicone spacer makes the behavior of bis-triazoles obtained more sensitive to the nature of the environment. The preliminary bioassay indicates lipophilic medium more suitable for biocide action of silicone-bridged bis-triazoles, which in some cases far exceeds that of reference. The mechanism of enzyme inhibition is demonstrated by molecular docking, and the results indicate that, in all docked complexes, the ligands are directly coordinated to the heme ferric iron.

1. Introduction

Methyl-substituted disiloxanes as well as oligomeric siloxanes, possess intrinsic structural features (high flexibility and hydrophobicity conferred by Si—O bond characteristics and by the presence of methyl groups attached to silicon atoms) and represent platforms available for chemical modification at the active sites with the view to obtain compounds with particular properties [1–3]. Several silanes and disiloxanes with terminal reactive groups are commercially available, and others can be easily obtained from appropriately substituted silanes through a hydrolysis-condensation sequence. In general, the reactive groups in disiloxanes are either Si—H functions or various organic groups (vinyl, chloro-, cyano-, carboxy-, glycidoxy-alkyl, *etc.*), which can be further modified by reactions specific to silicon (hydrosilylation) or organic (nucleophilic substitution, condensation, addition, *etc.*) chemistry, respectively. However, the conjugation of silicones with more polar species is often a challenge due to opposite polarities and differences in solubility and reactivity [4]. For example, the modification of siloxanes has been mainly performed to obtain compounds of technical interest such as liquid crystals [5], surfactants [6–8], anti-foaming and textile finishing agents [4], but only limited information is available so far for the applications of silicon-containing compounds as ligands, most of which has been reported by the authors of this work [9–19]. In addition, siloxanes have been employed as scaffolds in medicinal chemistry. Thus, several types of functional oligodimethylsiloxanes with a polar substituent (methylpyridinium, quaternary amino, phosphoramide, carboxyl, 1-alkyl-3-β-D-glucopyranosyl) at one chain end showed high transdermal penetration without irritation owing to the bulkiness and the physiological inertness of the siloxane backbone. Furthermore, it has been showed that the disiloxane compounds might limit inflammation even if it penetrated into the skin, because it remains in the stratum corneum due to its high lipophilicity, and no transfer into the epidermis occurs [20]. It is reported the application of 1-alkyl-3-β-D-glucopyranosyl-1,1,3,3-tetramethyldisiloxane and its oligomers as skin penetration enhancers [21]. The first imidazolophanes having bis(methylene) tetramethyldisiloxane spacers, which have been obtained by the reaction of 1,3-bis(iodomethyl)-1,1,3,3-tetramethyldisiloxane with imidazoles, have been reported to be useful as antibiotic and antitumor drugs, but also as building blocks for receptors and sensors, ionic liquids or molecular containers and catalysts [22]. A series of silanols, siloxanes or

* Corresponding author.
E-mail address: mcazacu@icmpp.ro (M. Cazacu).

https://doi.org/10.1016/j.molliq.2019.111560
0167-7322/

silanol-siloxanes having nucleobases attached through hydrocarbon chains with variable lengths has been synthesized, and one of these compounds inhibited HIV-1 replication in cell culture [23]. Also, another compound containing a 1,3-bis(methyl)tetramethyldisiloxane motif, namely 4-[(3-methoxyphenyl)-methyl]-2,2,6,6-tetramethyl-1-oxa-4-aza-2,6-disilacyclohexane hydrochloride, has been tested as skeletal muscle relaxant [24]. In the recent years, a project implemented by Harvard University aimed at the development and application of disiloxanes as a new class of hard anion-binding organocatalysts able to deliver medicinally important compounds in a new and highly specific way, an application that could help in the development and production of new compounds to fight cancer and other diseases [25]. Morpholino-disiloxane (ALIS-409) and piperazino-disiloxane (ALIS-421) have been developed as inhibitors of multidrug resistance of various types of cancer cells [26]. However, despite the aforementioned recent progress, there is still only scarce information on the biological activity of oligosiloxanes.

Heterocyclic compounds play an important role in our lives through their significance in all major life processes, their usefulness as scaffolds in the development of drugs, or as building blocks in materials with a wide range of applications. Within the broad field of heterocyclic compounds, 1,2,4-triazoles are a well-represented class of nitrogen-containing polyheteroatomic compounds with five-membered rings, which exhibit a broad spectrum of biological activities [27–37], while having low toxicity and good pharmacokinetic and pharmacodynamic profiles. Furthermore, in an approach towards the development of novel compounds based on different pharmacophores, it has been found that the presence of two or more pharmacological moieties in a molecule enhances the performance of the hybrid compound, which may bind to several active sites, and consequently exhibit higher bioactivity and therapeutic effect. Thus, derivatives of 1,2,3- and 1,2,4-triazoles were attached to methylene or ethylene bridges with a view to create a study base for the effect of the length of this bridge on the biological activity [38]. The presence of two triazole rings in the molecule could give the resulting compounds improved solubility in water, increased targeting capacity and higher bioactivity [39]. Despite the relatively low number of studies, the results obtained so far in this line of research validate the working hypothesis and constitute a motivation for further investigations.

In addition to biological activity, 1,2,4-triazoles have a remarkable potential for metal binding, as they form a wide variety of complexes that may differ in coordination number, geometry, or the number of metal ions in the coordinating unit. The presence in the structure of the three hard nitrogen donors that can easily coordinate the metal is responsible for the complex formation ability of 1,2,4-triazoles. Due to the position of these nitrogen atoms in the heterocyclic ring, 1,2,4-triazoles can also coordinate together [40,41] to afford complexes that could be of biological and medicinal interest [42]. Taking into account the above-mentioned considerations for 1,2,4-triazoles and silicones, it has been deemed interesting to connect multiple 1,2,4-triazole units using silicone spacers with the view to enhance the biological and metal bonding effects of the triazole moiety, and to generate novel properties due to the particular nature of the silicone segment (*e.g.*, high flexibility, hydrophobicity, low surface energy). Additionally, several flexible bis-triazole ligands based on organic spacers have been shown to be valuable candidates for building coordination polymers with different architectures [43], and this is most likely to be true for bis-triazole ligands derived from siloxane spacers as well.

Therefore, the present paper aims at derivatizing selected silanes and siloxanes in a telechelic manner with different 1,2,4-triazole derivatives to give the corresponding bis-triazoles. To the best of our knowledge, only a small number of similar structures have been mentioned so far in literature reports dealing mostly with medicinal or biological applications. Siloxane derivatives of triazoles have been not reported until 2016, when a study describing their preparation through the alkylation of triazoles with 1,3-bis(iodomethyl)-1,1,3,3-tetramethyldisiloxanes and presenting their characterization was published [44]. In our approach, bis(chloromethyl)dimethylsilane and 1,3-bis(chloromethyl)tetramethyldisiloxane were used as substrates and three mercaptotriazole derivatives were used as reagents in reactions leading to thioethers. Thioethers themselves constitute a class of valuable and significant compounds that are useful in heterocyclic synthesis, medicine, biochemistry, agriculture, industry, *etc.* [45,46]. The association of siloxanes with triazoles through a thioether bond represents a novel strategy for the creation of bis-triazole conjugates whose biological activity was subsequently assessed and interpreted from the perspective of the presence and the nature of the siloxane or silane spacer. The mechanism of enzyme inhibition has been demonstrated by molecular docking. The metal binding capacity was also evaluated both experimentally and theoretically by quantum mechanics.

2. Experimental

2.1. Materials

1,3-Bis(chloromethyl)-1,1,3,3-tetramethyldisiloxane (assay 99%, bp 204.5–205 °C, linear formula $ClCH_2Si(CH_3)_2OSi(CH_3)_2CH_2Cl$, MW 231.27, d^{25} 1.05 g/mL), and bis(chloromethyl)dimethylsilane (assay 97%, bp 159–160 °C, linear formula $(CH_3)_2Si(CH_2Cl)_2$, MW 157.11, d^{25} 1.075 g/mL), acetohydrazide (90%, molecular formula $C_2H_6N_2O$, MW 74.08, mp 58–68 °C), phenyl isothiocyanate (98%, molecular formula C_7H_5NS, MW 135.19), anhydrous potassium carbonate (K_2CO_3, powder, 99.99%, MW 138.21), copper(II) chloride dihydrate ($CuCl_2 \cdot 2H_2O$ 99.9%, MW 170.48) and *N*,*N*-dimethylformamide (DMF, p.a. 99.8%) were purchased from Sigma Aldrich. 3-Mercapto-1,2,4-triazole (>98.0%(GC)(T), molecular formula $C_2H_3N_3S$, MW 101.13, mp 218.0–223.0 °C) and 3-mercapto-4-methyl-1,2,4-triazole (>98.0%(T), molecular formula $C_3H_5N_3S$, MW 115.15, mp 165.0–169.0 °C) were purchased from TCI EUROPE N.V. and used as such. Abs. ethanol (p.a.), acetone (p.a.) chloroform (p.a.) and ethyl acetate (p.a.) were obtained from Chemical Company (Iaşi, Romania). Methanol (Emplura Grade, 98%) was provided by Merck Millipore.

3-Mercapto-4-phenyl-5-methyl-1,2,4-triazole **1** (molecular formula $C_9H_9N_3S$, MW 191.256) was prepared in a two-step reaction sequence comprising the addition of acethydrazide to phenyl isothiocyanate, followed by the ring closure of the resulting 2-acetyl-*N*-phenylhydrazine-1-carbothioamide in the presence of KOH, as described in the Experimental section.

The microorganisms required for the biological evaluation (*Aspergillus niger*, *Penicillium frequentans*, *Penicillium fumigatus*, *Alternaria alternate*, *Fusarium*, *Pseudomonas aeruginosa* and *Bacillus polymyxa*) were provided by American Type Culture Collection (ATCC), USA. Sabouraud agar medium with dextrose (4%, SDA) and Standard I nutrient agar medium were obtained from Merck (Schwalbach Hesse, Germany). Reference compounds caspafugin and kanamycin were from Liofilchem (Roseto degli Abruzzi, Italy).

2.2. Measurements

Fourier transform infrared (FT-IR) spectra were recorded using a Bruker Vertex 70 FT-IR spectrometer. The experiments were performed in the transmission mode in the range 400–4000 cm^{-1} at room temperature with a resolution of 2 cm^{-1} and accumulation of 32 scans. NMR spectra were recorded on a Bruker Avance NEO 400 MHz Spectrometer equipped with a 5 mm BBFO direct detection probe and z-gradients. The spectra were recorded in DMSO d_6 at room temperature, and the chemical shifts are reported as δ values (ppm) using the solvent residual peak (2.51 for ^1H and 39.5 for ^{13}C) as reference. Carbon, hydrogen, nitrogen and sulfur content were determined on a Perkin–Elmer CHNS 2400 II elemental analyser. Differential scanning calorimetry (DSC) measurements were performed on a DSC 200 F3 Maia (Netzsch, Germany) in the range − 150 ÷ 200 °C applying a heating and cooling rate of 10

°C/min. About 10 mg of sample were heated in pressed and punched aluminum crucibles using nitrogen as flowing inert purge gas at a flow rate of 100 mL/min. Melting points were taken on a MEL-TEMP capillary melting point apparatus and are uncorrected. UV–Vis absorption spectra measurements were carried out in methanol solution on a Specord 200 spectrophotometer.

2.2.1. X-ray crystallography

X-ray diffraction measurements for compounds **1**, **2** and **4** were carried out with an Oxford-Diffraction XCALIBUR E CCD diffractometer equipped with graphite-monochromated MoKα radiation. Single crystals were positioned at 40 mm from the detector and 392, and 395 frames were measured each for 30, and 70 s over 1° scan width for **2**, and **4**, respectively. Intensity data for **5**, **6** and **7** were collected with Oxford Diffraction SuperNova diffractometer using hi-flux micro-focus Nova CuKα (or MoKα radiation). The single crystal was positioned at 49 mm from the detector and 457, 430 and 463 frames were measured each for 50, 30 and 30 s over 1° scan width for **5**, **6** and **7**, respectively. The unit cell determination and data integration were carried out using the CrysAlis package of Oxford Diffraction [47]. The structures were solved by direct methods using Olex2 [48] software with the SHELXS structure solution program and refined by full-matrix least-squares on F^2 with SHELXL-97 [49] using an anisotropic model for non hydrogen atoms. All H atoms were introduced in idealised positions ($d_{CH} = 0.96$ Å) using the riding model. The positional parameters for H-atoms attached to O or N were verified by the geometric parameters of the possible hydrogen bonds. The molecular plots were obtained using the Olex2 program. The crystallographic data and refinement details are quoted in Table 1, while bond lengths are summarized in Table S1. CCDC-1847845 (**1**) CCDC-1846905 (**2**), CCDC-1846906 (**4**), CCDC-1846907 (**5**), CCDC–1846908 (**6**) and CCDC-1846909 (**7**) contain the supplementary crystallographic data for this contribution. These data can be obtained free of charge *via* www.ccdc.cam.ac.uk/conts/retrieving.html (or from the Cambridge Crystallographic Data Centre, 12 Union Road, Cambridge CB2 1EZ, UK; fax: (+44) 1223-336-033; or deposit@ccdc.ca.ac.uk).

2.3. Computational calculations

Two theoretical approaches have been combined to describe the mechanism of binding between the ligands (triazole derivatives) and the receptor (enzyme, 14α-Demethylase, *Aspergillus fumigatus*). The first theoretical procedure was based on quantum mechanics (QM) calculations and the second was the molecular docking. The QM calculations were employed to predict the structures, the dipole moment as well as the metal binding ability. The QM computations were based on *ab initio* method predicting the structure of metal chelating complexes. The Hartree-Fock (HF) functional was used with LanL2DZ basis set. All electronic calculations were carried out with Gaussian G09 program [50].

The dipole moment of triazole derivatives and their metal binding capacity were also evaluated with HF/Lan2DZ level of theory. The binding energy of metal-ligand complex (ML) was computed on equilibrium geometries by the following formula:

$$E_{bind}M{-}L = E(M{-}L\ complex) - \left(\mathrm{E}\left(M^{2+}\right) + E(L)\right)$$

where $E(M\text{-}L\ complex)$ would be the energy of the whole metal complex, $E(M^{2+})$ is the energy of the metal cation, $E(L)$ is the energy of the ligands silicone bis-triazoles ligand without metal (L(7)).

The molecular docking was performed with AutoDock 4.2 software package [51]. The number of docking trials was set to 1000 poses, while ligand structure was kept flexible in order to obtain more conformations with low energies. The molecular docking simulations were repeated to confirm that the results are reproducible. The initial ligands structures were obtained from crystallographic data. The 14α-Demethylase (*Aspergillus fumigatus*) was selected as the target enzyme and was taken from the Protein Data Bank (PDB) code 6CR2 [52]. The ligand-enzyme complex with the lowest K_d was selected as the most probable binding mode for each compound. Because the parametrization for Si atom is missing from AutoDock, the empirical parameters for this atom were taken over from carbon (which it is isoelectronic

Table 1
Crystal data and details of data collection.

Compound	**1**	**2**	**4**	**5**	**6**	**7**
Empirical formula	$C_9H_9N_3S$	$C_{24}H_{32}N_6OS_2Si_2$	$C_{10}H_{20}N_6OS_2Si_2$	$C_{23.5}H_{33.5}N_{6.5}O_{1.5}S_2Si$	$C_{10}H_{18}N_6S_2Si$	$C_8H_{14}N_6S_2Si$
Fw	191.25	540.86	360.62	523.28	314.51	286.46
T [K]	294	293	200	293	293	293(2)
Crystal system	Triclinic	Triclinic	Triclinic	Orthorhombic	Orthorhombic	Trigonal
Space group	*P*-1	*P*-1	*P*-1	$Pmn2_1$	*Pnam*	*R*-3
a [Å]	6.8845(7)	9.2110(11)	8.0129(5)	21.445(4)	11.8768(12)	27.3748(16)
b [Å]	7.3728(8)	12.3774(14)	8.9536(7)	10.1967(17)	6.8522(5)	27.3748(16)
c [Å]	10.3138(9)	14.0350(16)	13.9206(12)	6.6078(14)	19.8637(19)	9.8198(6)
α [°]	96.909(8)	73.983(10)	79.051(7)	90.00	90.00	90.00
β [°]	93.589(8)	74.816(10)	84.366(6)	90.00	90.00	90.00
γ [°]	107.554(10)	71.495(10)	70.593(7)	90.00	90.00	120.00
V [Å^3]	492.79(9)	1431.5(3)	924.16(12)	1444.9(5)	1616.5(3)	6372.9(7)
Z	2	2	2	2	4	18
ρ_{calcd} [g cm^{-3}]	1.289	1.255	1.296	1.203	1.292	1.344
μ [mm^{-1}]	0.284	0.298	0.425	0.255	0.400	4.145
Crystal size [mm]	0.30 × 0.30 × 0.02	0.30 × 0.20 × 0.05	0.20 × 0.06 × 0.02	0.30 × 0.15 × 0.03	0.20 × 0.05 × 0.02	0.25 × 0.01 × 0.01
Radiation	MoKα (λ = 0.71073)	MoKα (λ = 0.71073)	MoKα (λ = 0.71073)	MoKα (λ = 0.71073)	MoKα (λ = 0.71073)	CuKα (λ = 1.54184)
2Θ range	4 to 48.814	3.08 to 50.04	2.98 to 50.04	6.46 to 50.06	6.28 to 50.06	21.8 to 141
Reflections collected	3068	9658	6374	10,204	10,430	4630
Independent reflections	1613 [R_{int} = 0.0356]	5029 [R_{int} = 0.0422]	3270 [R_{int} = 0.0349]	2597 [R_{int} = 0.0708]	1467 [R_{int} = 0.0458]	2625 [R_{int} = 0.0399]
Data/restraints/parameters	1613/0/119	5029/0/322	3270/0/194	2597/8/166	1467/0/94	2625/0/160
R_1[a]	0.0891	0.0734	0.0549	0.0691	0.0584	0.0467
wR_2[b]	0.2470	0.1556	0.1142	0.1952	0.1653	0.1045
GOF[c]	1.102	1.064	1.062	1.028	1.030	1.031
Largest diff. peak/hole/e Å^{-3}	0.68/−0.26	0.33/−0.21	0.31/−0.33	0.44/−0.35	0.30/−0.24	0.23/−0.23

[a] $R_1 = \Sigma||F_o|-|F_c||/\Sigma|F_o|$.
[b] $wR_2 = \{\Sigma[w(F_o^2-F_c^2)^2]/\Sigma[w(F_o^2)^2]\}^{1/2}$.
[c] GOF = $\{\Sigma[w(F_o^2-F_c^2)^2]/(n-p)\}^{1/2}$, where n is the number of reflections and p is the total number of parameters refined.

with Si atom), except the charges (Gasteiger) and the van der Waals parameters, which were computed in accordance with the AutoDock 4.2 methodology.

2.4. Synthesis

2.4.1. 3-Mercapto-4-phenyl-5-methyl-1,2,4-triazole, **1**

To a solution of acethydrazide (814 mg, 10 mmole, 90% purity) in abs. ethanol (10 mL), phenyl isothiocyanate (1.35 g, 10 mmole) was added. The mixture was heated at reflux temperature for 1 h, it was allowed to cool at room temperature, and then it was refrigerated for 3 h. The crystalline material was filtered, sequentially washed with cold isopropanol (2 × 5 mL) and hexanes (1 × 10 mL), and air-dried. The resulting 2-acetyl-*N*-phenylhydrazine-1-carbothioamide (1.96 g, 9.38 mmole) was added to a solution of KOH (741 mg, 11.25 mmole, 85% purity) in water (30 mL), and the mixture was heated at reflux temperature for 3 h. The cold reaction mixture was filtered, and then the filtrate was treated dropwise under efficient stirring with 10% HCl until pH 2. The solid material was filtered, washed thoroughly with water, air-dried and recrystallized to give colorless crystals (1.415 g, 79%), mp 214–215 °C (ethanol). IR spectrum (KBr pellet), ν_{max}: 3099s, 3051s, 2916s, 2906s, 2758m, 2729s, 1582m, 1501vs. ^{1}H NMR, (400.13 MHz, δ (ppm), DMSO-d_6): 13.65 (s, 1H, NH), 7.59–7.42 (m, 5H, aromatic protons), 2.09 (s, 3H, CH_3). ^{13}C NMR, (100.6 MHz, δ (ppm), DMSO-d_6): 167.4 (C=S), 149.1 (C-CH_3), 133.8 (C—N), 129.3, 128.1 (aromatic carbon atoms), 11.7 (CH_3). *Anal.* Calcd. for $C_9H_9N_3S$ (M = 191.25 g/mol), %: C, 56.52; H, 4.74; N, 21.97; S, 16.77. Found: C, 56.34; H, 4.52; N, 21.85; S, 16.87.

2.4.2. 1,1,3,3-Tetramethyl-1,3-bis{[(5-methyl-4-phenyl-4H-1,2,4-triazol-3-yl)thio]methyl}disiloxane, **2**

A solution of 1,3-bis(chloromethyl)tetramethyldisiloxane (0.18 g, 0.78 mmole) in acetone (2.5 mL) was added to the solution of 3-mercapto-4-phenyl-5-methyl-1,2,4-triazole **1** (0.30 g, 1.56 mmole) in acetone (4.5 mL). Anhydrous K_2CO_3 (0.24 g, 1.72 mmole) was then added, and the mixture was heated at reflux temperature for 5 h. Then, the inorganic salts were filtered off, and crystals of compound **2** gradually separated from the filtrate as acetone slowly evaporated. The crystals were filtered, washed with methanol and dried. Yield 0.35 g (83%). T_m 131 °C (DSC peak), Tg 2 °C. UV–vis (methanol, 3.8 × 10^{-5} M): λ_{max} (ε, M^{-1} cm^{-1}) 248 (16563). IR (KBr): ν_{max} 3059w, 2960m, 2904w, 2374w, 1595m, 1533m, 1498s, 1433s, 1384s, 1317m, 1257s, 1134w, 1060vs, 839vs, 808vs, 727w, 694s, 555m. ^{1}H NMR (DMSO-d_6, 400.13 MHz,): δ (ppm) 7.61–7.42 (m, 10H, aromatic protons), 2.35 (s, 4H, S-CH_2-Si), 2.19 (s, 6H, triazole-CH_3), 0.06 (s, 12H, Si-CH_3). ^{13}C NMR (DMSO-d_6, 100.6 MHz,): δ (ppm) 152.3 (C-CH_3), 151.0 (C—S from triazole), 133.2 (C—N from phenyl), 129.9–127.0 (5 aromatic carbons), 17.6 (S-CH_2-Si), 10.8 (triazole-CH_3), −0.2 (Si-CH_3). *Anal.* Calcd. for $C_{24}H_{32}N_6OS_2Si_2$ (M = 540.86 g/mol), %: C, 53.30; H, 5.96; N, 15.54; S, 11.86. Found: C, 53.55; H, 5.99; N, 15.50; S, 11.91.

2.4.3. 1,1,3,3-Tetramethyl-1,3-bis{[(4-methyl-4H-1,2,4-triazol-3-yl)thio]methyl}disiloxane, **3**

A solution of 1,3-bis(chloromethyl)tetramethyldisiloxane (0.18 g, 0.78 mmole) in acetone (2.5 mL) was added to the solution of 3-mercapto-4-methyl-1,2,4-triazole (0.18 g, 1.56 mmole) in acetone (4.5 mL). Anhydrous K_2CO_3 (0.24 g, 1.72 mmole) was then added, and the mixture was heated at reflux temperature for 5 h. Afterwards, the inorganic salts were filtered off, and the filtrate was allowed to slowly evaporate to afford a residue which was dissolved in chloroform. The resulting solution was repeatedly extracted with water (3 × 10 mL), dried over anh. Na_2SO_4, and allowed to slowly evaporate to give a crystalline material. Yield 0.22 g (72%). T_m 104 °C (DSC peak), Tg −30 °C. UV–vis (methanol, 4.28 × 10^{-5} M): λ_{max} (ε, M^{-1} cm^{-1}) 249 (9539). IR (KBr): ν_{max} 3109w, 3012vw, 2956m, 2904w, 1649w, 1562vw, 1512s, 1473m, 1421s, 1365m, 1257vd, 1201m, 116m, 1132w, 1066vs, 954w, 906w, 842vs, 808vs, 754w, 694m, 648m, 532w. ^{1}H NMR (DMSO-d_6, 400.13 MHz,): δ (ppm) 8.55 (s, 2H, CH from triazole), 3.56 (s, 6H, N-CH_3 overlapped with the residual peak of water from solvent), 2.47 (s, 4H, S-CH_2-Si), 0.20 (s, 12H, Si-CH_3). ^{13}C NMR (DMSO-d_6, 100.6 MHz,): δ (ppm) 150.7 (C—S from triazole), 146.0 (CH from triazole), 30.6 (N-CH_3), 18.1 (S-CH_2-Si), −0.1 (Si-CH_3). *Anal.* Calcd. for $C_{12}H_{24}N_6OS_2Si_2$ (M = 388.659 g/mol),%: C, 37.08; H, 6.22; N, 21.62; S, 16.50. Found: C, 37.34; H, 6.27; N, 21.78; S, 16.76.

2.4.4. 1,3-Bis{[(4H-1,2,4-triazol-3-yl)thio]methyl}-1,1,3,3-tetramethyldisiloxane, **4**

A solution of 1,3-bis(chloromethyl)tetramethyldisiloxane (0.18 g, 0.78 mmole) in acetone (2.5 mL) was added to the solution of 3-mercapto-1,2,4-triazole (0.16 g, 1.56 mmole) in acetone (4.5 mL). Anhydrous K_2CO_3 (0.24 g, 1.72 mmole) was then added, and the mixture was heated at reflux temperature for 5 h. After the inorganic salts were filtered off, compound **4** was isolated from the filtrate and purified in a manner similar to the one described for compound **3**. Yield 0.23 g (79%). T_m 110 °C (DSC peak), Tg −15 °C. UV–vis (methanol, 4.62 × 10^{-5} M): λ_{max} (ε, M^{-1} cm^{-1}) 236 (14653). IR (KBr): ν_{max} 3103w, 2958m, 2902m, 1645w, 1521w, 1458s, 1396w, 1338m, 1257vs, 1182m, 1136w, 1066vs, 898w, 839vs, 806vs, 756w, 707w, 497w. ^{1}H NMR (DMSO-d_6, 400.13 MHz,): δ (ppm) 13.93 (s, 2H, NH), 8.34 (s, 2H, CH from triazole), 2.42 (s, 4H, S-CH_2-Si), 0.18 (s, 12H, Si-CH_3). ^{13}C NMR (DMSO-d_6, 100.6 MHz,): δ (ppm) 158.2 (C—S from triazole), 146.5 (CH from triazole), 17.2 (S-CH_2-Si), −0.1 (Si-CH_3). *Anal.* Calcd. for $C_{10}H_{20}N_6OS_2Si_2$ (M = 360.606 g/mol), %: C, 33.31; H, 5.59; N, 23.31; S, 17.78. Found: C, 33.45; H, 5.83; N, 23.45; S, 17.32.

2.4.5. Dimethylbis{[(5-methyl-4-phenyl-4H-1,2,4-triazol-3-yl)thio]methyl}silane, **5**

A solution of bis(chloromethyl)dimethylsilane (0.12 g, 0.78 mmole) in acetone (2.5 mL) was added to the solution of 3-mercapto-4-phenyl-5-methyl-1,2,4-triazole **1** (0.30 g, 1.56 mmole) in acetone (4.5 mL). Anhydrous K_2CO_3 (0.24 g, 1.72 mmole) was then added, and the mixture was heated at reflux temperature for 5 h. The inorganic salts were filtered off, and then the filtrate was allowed to slowly evaporate. The resulting residue was dissolved in a warm mixture of ethyl acetate: DMF (2.5 mL, 1:10 *v*/*v*), then the solution was brought to room temperature. The product crystallized in a few hours, and it was filtered off, rapidly washed with a small volume of ethyl acetate and dried. Yield 0.29 g (81%). T_m 136 °C (DSC peak), Tg −17 °C. UV–vis (methanol, 5.8 × 10^{-5} M): λ_{max} (ε, M^{-1} cm^{-1}) 256 (19406). IR (KBr): ν_{max} 3055w, 2955 m, 2903 m, 2747w, 1709vs, 1589s, 1533m, 1499vs, 1423s, 1319s, 1256s, 1045s, 916w, 841s, 772s, 729m, 694s, 609w, 557m, 500w. ^{1}H NMR (DMSO-d_6, 400.13 MHz,): δ (ppm) 7.60–7.42 (m, 10H, aromatic protons), 2.43 (s, 4H, S-CH_2-Si), 2.18 (s, 6H, triazole-CH_3), 0.06 (s, 6H, Si-CH_3). ^{13}C NMR (DMSO-d_6, 100.6 MHz,): δ (ppm) 152.9 (C-CH_3), 151.3 (C—S from triazole), 133.7 (C—N from phenyl), 129.9–127.0 (5C, aromatic carbons), 15.4 (S-CH_2-Si), 11.3 (triazole-CH_3), −3.5 (Si-CH_3). *Anal.* Calcd. for $C_{47}H_{67}N_{13}O_3S_4Si_2$ (M = 1046.58 g/mol), %: C, 53.94; H, 6.45; N, 17.40; S, 12.26. Found: C, 54.41; H, 6.70; N, 17.75; S, 12.65.

2.4.6. Dimethylbis{[(4-methyl-4H-1,2,4-triazol-3-yl)thio]methyl}silane, **6**

A solution of bis(chloromethyl)dimethylsilane (0.12 g, 0.78 mmole) in acetone (2.5 mL) was added to the solution of 3-mercapto-4-methyl-1,2,4-triazole (0.18 g, 1.56 mmole) in acetone (4.5 mL). Anhydrous K_2CO_3 (0.24 g, 1.72 mmole) was then added, and the mixture was heated at reflux temperature for 5 h. The inorganic salts were filtered off, and the filtrate was processed in a manner similar to the one described for compound **5** to give bis-triazole **6**. Yield 0.21 g (85%). T_m 146 °C (DSC peak), Tg −18 °C. UV–vis (methanol, 5.29 × 10^{-5} M): λ_{max} (ε, M^{-1} cm^{-1}) 250 (19024). IR (KBr): ν_{max} 3859w, 3742w, 3627w, 3564w, 3096m, 3007m, 2957m, 2908w, 2355w, 1653w, 1558w, 1528s, 1472s, 1418s, 1362s, 1254s, 1213s, 1159m, 1067s,

991w, 955w, 833vs, 725m, 690m, 648m, 432w. ^{1}H NMR (DMSO-d_6, 400.13 MHz,): δ (ppm) 8.53 (s, 2H, CH from triazole), 3.57 (s, 6H, N-CH_3), 2.55 (s, 4H, S-CH_2-Si), 0.18 (s, 6H, Si-CH_3). ^{13}C NMR (DMSO-d_6, 100.6 MHz,): δ (ppm) 150.4 (C—S from triazole), 146.1 (CH from triazole), 30.6 (N-CH_3), 15.6 (S-CH_2-Si), −4.1 (Si-CH_3). *Anal.* Calcd. for $C_{10}H_{18}N_6S_2Si$ (314.505 g/mol), %: C, 38.19; H, 5.77; N, 26.72; S, 20.39. Found: C, 38.52; H, 5.43; N, 27.01; S, 20.72.

2.4.7. Bis{[(4H-1,2,4-triazol-3-yl)thio}methyl}dimethylsilane, **7**

A solution of bis(chloromethyl)dimethylsilane (0.12 g, 0.78 mmole) in acetone (2.5 mL) was added to the solution of 3-mercapto-1,2,4-triazole (0.16 g, 1.56 mmole) in acetone (4.5 mL). Anhydrous K_2CO_3 (0.24 g, 1.72 mmole) was then added, and the mixture was heated at reflux temperature for 5 h. The inorganic salts were filtered off to give a filtrate that was processed in a manner similar to the one described above for compound **5** to afford bis-triazole **7**. Yield 0.18 g (82%). T_m 167 °C (DSC peak), Tg −7 °C. UV–vis (methanol, 3.49×10^{-5} M): λ_{max} (ε, M^{-1} cm^{-1}): 243 (16143). IR (KBr): ν_{max} 3851vw, 3782vw, 3638w, 3574w, 3117s, 2944m, 2904m, 1659w, 1516m, 1464s, 1404m, 1344vs, 1256vs, 1178m, 1134w, 1051m, 1005w, 966w, 845vs, 760w, 698m, 636w, 500w, 407vw. ^{1}H NMR (DMSO-d_6, 400.13 MHz,): δ (ppm) 8.29 (s, 2H, CH from triazole), 7.38 (s, 2H, NH), 2.48 (s, 4H, S-CH_2-Si), 0.15 (s, 6H, Si-CH_3). ^{13}C NMR (DMSO-d_6, 100.6 MHz,): δ (ppm) 157.8 (C—S from triazole), 146.9 (CH from triazole), 14.7 (S-CH_2-Si), −3.9 (Si-CH_3). *Anal.* Calcd. for $C_8H_{14}N_6S_2Si$ (286.452 g/mol), %: 33.54; H, 4.93; N, 29.34; S, 22.39. Found: C, 33.89; H, 5.20; N, 28.98; S, 22.77.

2.5. Assessment of metal binding capacity

In order to investigate the complex formation ability of the newly synthesized compounds, stock solutions of bis-triazole derivatives **2**–**7** (0.1 mM) in methanol and $CuCl_2 \cdot 2H_2O$ (1 mM) in methanol were prepared. In titration experiments, increasing volumes (containing up to 10 equivalents of $CuCl_2 \cdot 2H_2O$) of diluted metal ion solution in methanol were sequentially added into the solution of the bis-triazole derivatives. The samples were mixed at room temperature prior to each UV–vis measurement. Spectra were recorded in the 200–400 nm spectral range at room temperature.

2.6. Assessment of antimicrobial activity

Antibacterial and fungicidal activity was evaluated by performing *in vitro* tests against pure culture of five fungi species, one Gram-negative and one Gram-positive bacteria. Antimicrobial evaluation was performed by the MIC test strip method according to standard procedures [53]. Cultivation was performed by using a mixture of 1:1 microorganism suspension and solution of the compound to be tested that were placed on the solid medium. When the MIC Test Strip is applied onto an inoculated agar surface, the preformed exponential gradient of antimicrobial agent is immediately transferred to the agar matrix. After 48 h of incubation a symmetrical inhibition ellipse centered along the strip was formed. The MIC value is read directly from the scale as μg/mL at the point where the edge of the inhibition ellipse of intersects with the MIC test strip. Observations on the results were made by visual analysis and microscopy, using a Novex stereomicroscope Ap-8 Euromex (Olympus Europa Holding GmbH, Hamburg, Germany) and Olympus SZY 160 microscope (Olympus Corporation, Shinjuku, Tokyo, Japan). MIC Test Strip is a quantitative assay for determining the Minimum Inhibitory Concentration MIC of antimicrobial agents against microorganisms and for detecting the resistance mechanisms [53]. It should be noted that Sabouraud agar medium with dextrose (4%, SDA) was used for fungi, while a Standard I nutrient agar medium was used for bacteria.

3. Results and discussion

3.1. Synthesis of bis-triazoles and structural analysis

Alkylation of thiols with alkyl halides is a well-known method for the formation of thioethers. This paper reports the *S*-alkylation of three mercaptotriazoles, namely 3-mercapto-1,2,4-triazole, 3-mercapto-4-methyl-1,2,4-triazole, and 3-mercapto-4-phenyl-5-methyl-1,2,4-triazole with two silicon-containing alkylating agents, namely 1,3-bis(chloromethyl)-1,1,3,3-tetramethyldisiloxane and bis(chloromethyl)dimethylsilane (Scheme 1). While all other reagents were purchased from the market, 3-mercapto-4-phenyl-5-methyl-1,2,4-triazole was synthesized and characterized in the laboratory (Figs. S1–S4). The thioalkylation reactions were conducted in the presence of K_2CO_3 in acetone at reflux temperature. Acetone, rather than DMF (another solvent recommended for such reactions [54]), was the solvent we chose owing to its good miscibility with siloxanes/silicones.

The progress of the *S*-alkylation reaction was monitored by IR spectroscopy. Thus, the decrease in intensity and, finally, the disappearance of the absorption band corresponding to the S—H bond in mercaptotriazole at around 2620 cm^{-1}, corroborated with the disappearance of the absorption band for the C—Cl bond in chloromethyl-terminated silicones at approximately 750 cm^{-1}, was indicative for the gradual advance of the reaction to completion. In the same manner, the increase in intensity of the S—C band around 550–560 cm^{-1} was suggestive for the formation of thioethers **2**–**7**. Additional evidence for the conversion of mercaptotriazole into the corresponding thioether is the modification of the IR absorption pattern for C—H stretch band of the triazole ring or, for compounds **1** and **2**, from the phenyl ring. In the case of the starting mercaptotriazoles, this pattern consists of two bands around 3000–3100 cm^{-1} (3051 and 3100 cm^{-1} in the case of 3-mercapto-4-phenyl-5-methyl-1,2,4-triazole, 3117 and 3165 cm^{-1} in the case of 3-mercapto-4-methyl-1,2,4-triazole, 3084 and 3144 cm^{-1} in the case of 3-mercapto-1,2,4-triazole) that correspond to the two tautomeric forms (thiol and thione) of this particular type of compounds. The aromatic C—H stretch appears as a single band for the corresponding thioethers lacking the possibility of tautomerism (3046, 3109, 3103, 3055, 3115, and 3117 cm^{-1} in the case of compound **2**, **3**, **4**, **5**, **6**, and **7**, respectively) (for more, see ESI). Once the reaction was complete, the inorganic salts were filtered off, and the reaction product was isolated from the filtrate by different procedures, depending on the structure of the product. Thus, compound **2** was separated directly in crystalline form from the filtrate by slow evaporation of the solvent, while in other cases (compounds **3** and **4**), the isolation of the product consisted in the evaporation of acetone, followed by repeated extractions with water of the solution of the resulting residue in chloroform in order to completely remove the inorganic salts. A crystalline product separated from the chloroform solution after slow evaporation of the solvent. Silane derivatives **5**–**7** crystallize well from ethyl acetate in the presence of a few drops of DMF. The yields range from good to excellent, and purity of the separated products was high, as shown by the results of the elemental analysis (*vide supra*). The chemical shift of the peaks in the ^{1}H and ^{13}C NMR spectra, along with the integral ratios of the peaks from the ^{1}H NMR spectra, confirm that the proposed structures for compounds **2**–**7** are correct. Also, the correlation between the triazole carbon attached to sulfur (151–158 ppm) and the protons in the methylene group adjacent to sulfur (2.35–2.55 ppm) in the H,C-HMBC spectra for compounds **2**–**7** indicates that the reactions took place with the formation of a novel covalent bond between the sulfur atom in mercaptotriazoles and the terminal carbon atom in the silicones used as starting materials (Figs. S5–S22).

DSC scans in the temperature range of −150 ÷ 200 °C, which have been performed for all the newly synthesized compounds, revealed a melting endotherm (T_m) along with a clear, second order transition assigned to the glass transition (T_g). In the case of bis-triazoles **2**–**7**, the observed glass transitions could be tentatively explained, on one

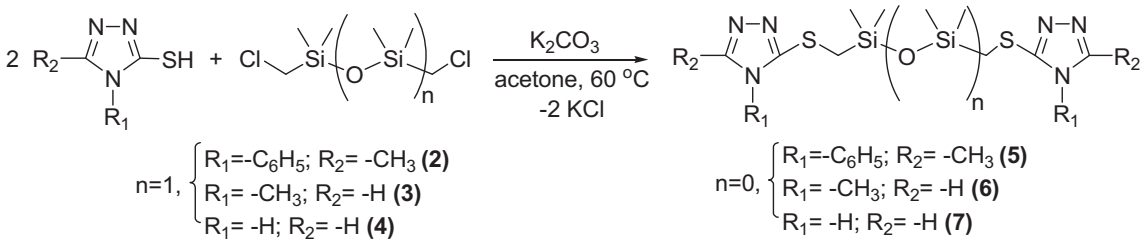

Scheme 1. Alkylation reaction of 3-mercapto-1,2,4-triazole derivatives with 1,3-bis(chloromethyl)-1,1,3,3-tetramethyldisiloxane and bis(chloromethyl)dimethylsilane leading to compounds **2**–**7**.

hand, by the presence of the seven-atom long spacer between the triazole rings for the siloxane derivatives **2**–**4** and of the five atom bridges for silanes **5**–**7**, and, on the other hand, by the crystal packing of these compounds (*vide infra*) in extended structures (one-, two- or three-dimensional) either through hydrogen bonds (case of the compounds **4**, **6** and **7**) or intermolecular π-π stacking (compound **5**). However, Tg glass transition also occurs in the case of compound **2**, whose crystal structure has been found to be composed of discrete molecules that interact poorly. Consequently, it seems that the presence of the spacer is the main cause for the detected glass transitions, a conclusion that is supported by the observation that, with the exception of value recorded for compound **2**, all the values of Tg are negative, ranging between −7 and −30 °C, and this is specific for highly flexible silicones. Low Tg values are associated with an increased difficulty in obtaining crystalline materials, as was the case for compound **3** (Tg −30 °C), for which it was not possible to isolate a suitable crystal for an accurate structural analysis. As expected, melting temperatures are lower than those of the starting triazoles, and range from 104 °C (compound **3**) to 167 °C (compound **7**). It is noteworthy that silane derivatives have higher melting temperatures than their siloxane counterparts.

3.1.1. Crystallographic analysis

The results of X-ray diffraction study of the precursor **1** and the compounds **2**–**7** are shown in Figs. 1–7, while bond distances and angles are listed in Table S1. All the studied compounds have a molecular crystal structure, which is built up from the corresponding neutral molecules without any co-crystallized solvent molecules except the compound **5**, which crystalizes with DMF and H_2O molecules in 1:0.5:1 ratio.

As shown in Fig. 1, in the crystal state the molecule **1** exhibit essentially non-planar configuration with the dihedral angle between triazole and phenyl rings at 75.7(3)°. The crystal structure is built from the dimeric supramolecular units (Fig. 2) formed *via* hydrogen bonding between N—H group of triazole system as donor and sulfur atom of adjacent molecule, as acceptor of proton.

In compounds **2** and **4**, the central part of the molecules is formed by a tetramethyldisiloxane fragment (Fig. 3) showing close geometric parameters. The average Si—O distance and Si-O-Si angles are of 1.626 (4) Å, 1.624(3) Å and 152.5(2)°, 155.7(2)°, for **2** and **4**, respectively. Due to high flexibility of the spacer, such compounds could adopt either *trans* or *cis* conformations as it was found in the case of ethane or propane spacers [55]. According to X-ray crystallography, molecule **2** has a *trans*-oid configuration (Fig. 3a), while **4** has a *cis*-oid configuration, which is stabilized by the intramolecular stacking interaction between triazole rings at 3.56 Å of centroid-to-centroid distance (Fig. 3b). In the case of compound **2**, the π-π triazole interaction is not possible due to the presence of phenyl substituents, which are not in the same plane as the triazole rings. Obviously, the adoption of a particular conformation affects the packaging in the crystalline structure. The crystal structure of compound **2** can be characterized as the packing of discrete, weakly interacting molecules. In opposition to this, the crystal packing for compound **4** shows the presence of one-dimensional supramolecular chains due to fragments that are potential proton donors or proton acceptors. A view of the main crystal structure motif in the crystal **4**, consolidated by N-H—N hydrogen-bonds is depicted in Fig. 4.

In an effort to elucidate the crystal structure of compound **3**, its crystallization from a large variety of mixed solvents has been repeatedly attempted. Unfortunately, all the experiments gave only a bunch of small-sized polycrystalline products unsuitable for single-crystal X-ray diffraction studies. All of the tested crystals were weakly diffracting with quite low resolution, and the reciprocal space has clearly showed the

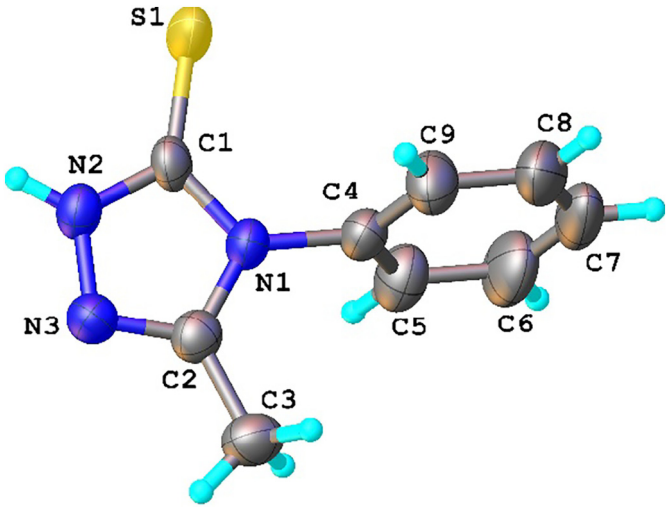

Fig. 1. X-ray molecular structure of **1** with atom labeling and thermal ellipsoids at 50% probability.

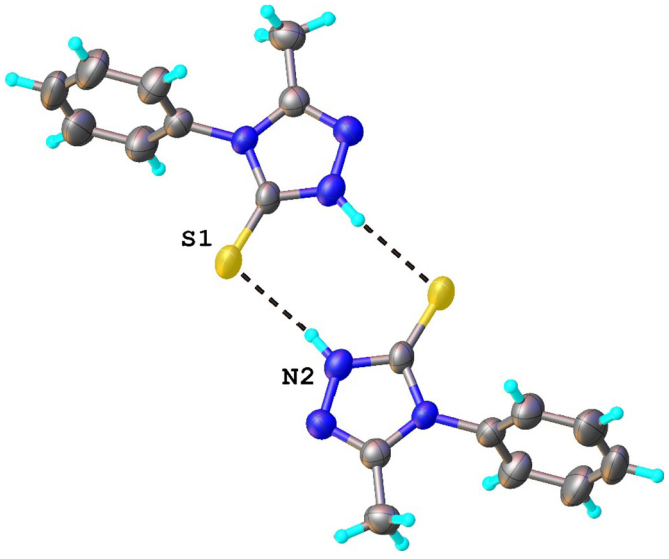

Fig. 2. Dimeric associate in the crystal structure **1**. H-bond parameters: N2-H—S1 [N2—H 0.86 Å, H—S1 2.42 Å, H—S1(1 –*x*, 2 – *y*, 1 - -*z*) 3.274(4) Å, ∠ N2HS1 173.6°.

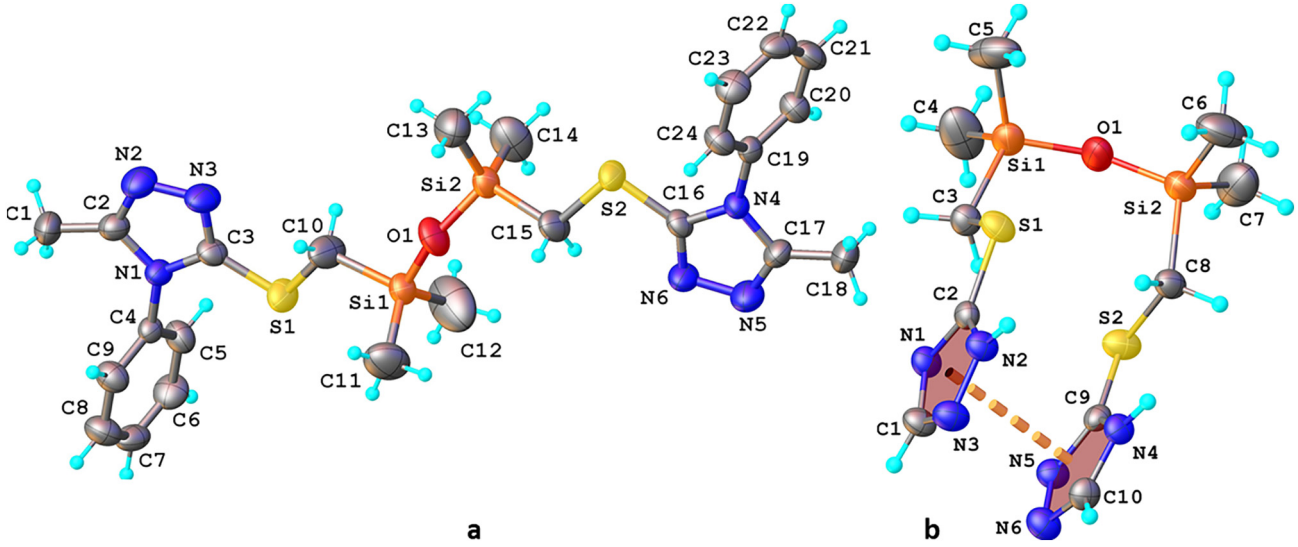

Fig. 3. X-ray molecular structure of compounds **2** (a) and **4** (b) with atom labeling scheme and thermal ellipsoids at 540% probability. Centroid-to-centroid contact is shown in orange-dashed line.

presence of an aggregate of several crystalline grains. Nevertheless, the structure could be solved and the electron density of the molecule was well defined, allowing the determination of the atomic connectivity. The model of the structure was refined with anisotropic temperature factors for all non hydrogen atoms (see Fig. S23 and exp_532.res file SI). The model proposed on the basis of these attempts is supported by the results of complementary analysis (elemental, IR, NMR). The structure of this compound was also designed and optimized towards reached to equilibrium structure (Fig. S24), level of theory for optimization procedure being that described in Computational calculations section.

The asymmetric parts of the crystal structures of compounds **5**, **6** and **7**, containing the dimethylsilane fragment are depicted in Fig. 5a, b and c, respectively. The bond lengths and angles are summarized in Table S1.

In the crystals of **5** and **6**, the packing of the neutral molecules shows the presence of two-dimensional supramolecular network, as depicted in Fig. 6a and b, respectively. In the case of compound **5**, 2D layers are formed due to the intermolecular π-π stacking between centrosymmetrically related triazole rings at 3.447 Å (Fig. 6a). In the crystal of **6**, the formation of the wave-like 2D network is driven by C-H—N intermolecular hydrogen bonding (Fig. 6b). A partial view of the crystal structure of **7** along *c* crystallographic axis is shown in Fig. 7. In this case, the packing diagram can be characterized as a three-dimensional supramolecular motif, based on the hydrogen bonding involving N—H

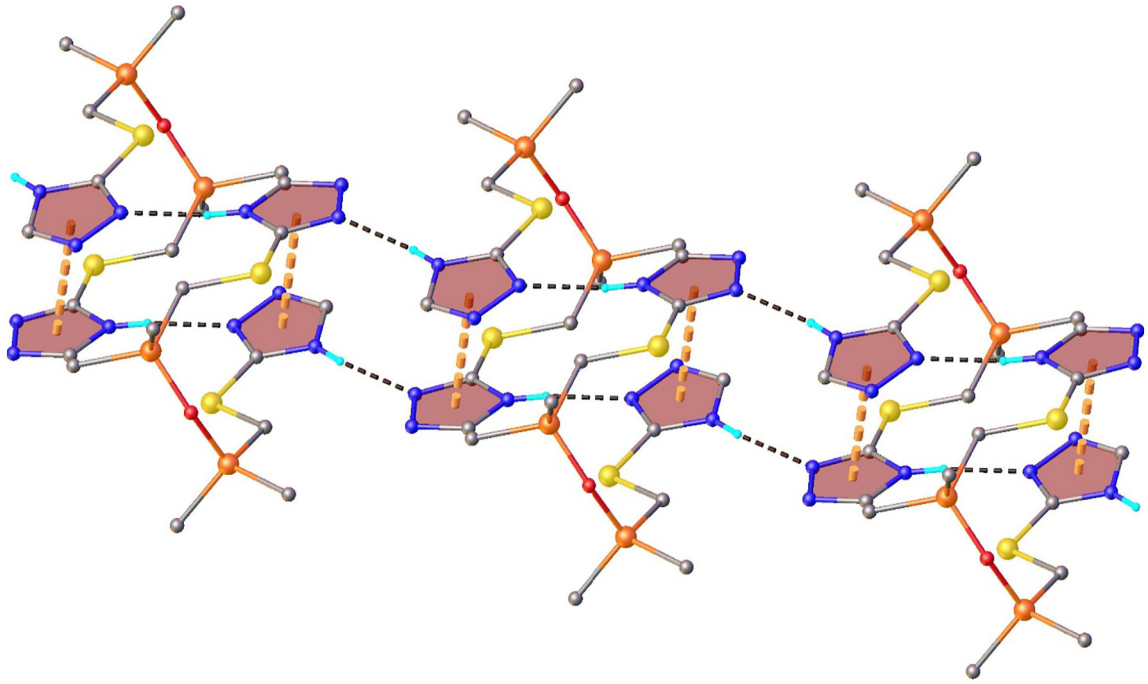

Fig. 4. One-dimensional supramolecular architecture in the crystal structure **4**. H-bonds parameters: N1-H—N2 [N1—H 0.86 Å, H—N1 2.01 Å, N1—N2(1 - *x*, -*y*, 1 – *z*) 2.855(4) Å, ∠N1HN2 167.5°]; N2-H—N5 [N2—H 0.86 Å, H—N5 2.02 Å, N2—N5(-*x*, 1 -*y*, 1 – *z*) 2.856(4) Å, ∠N2HN5 162.7°].

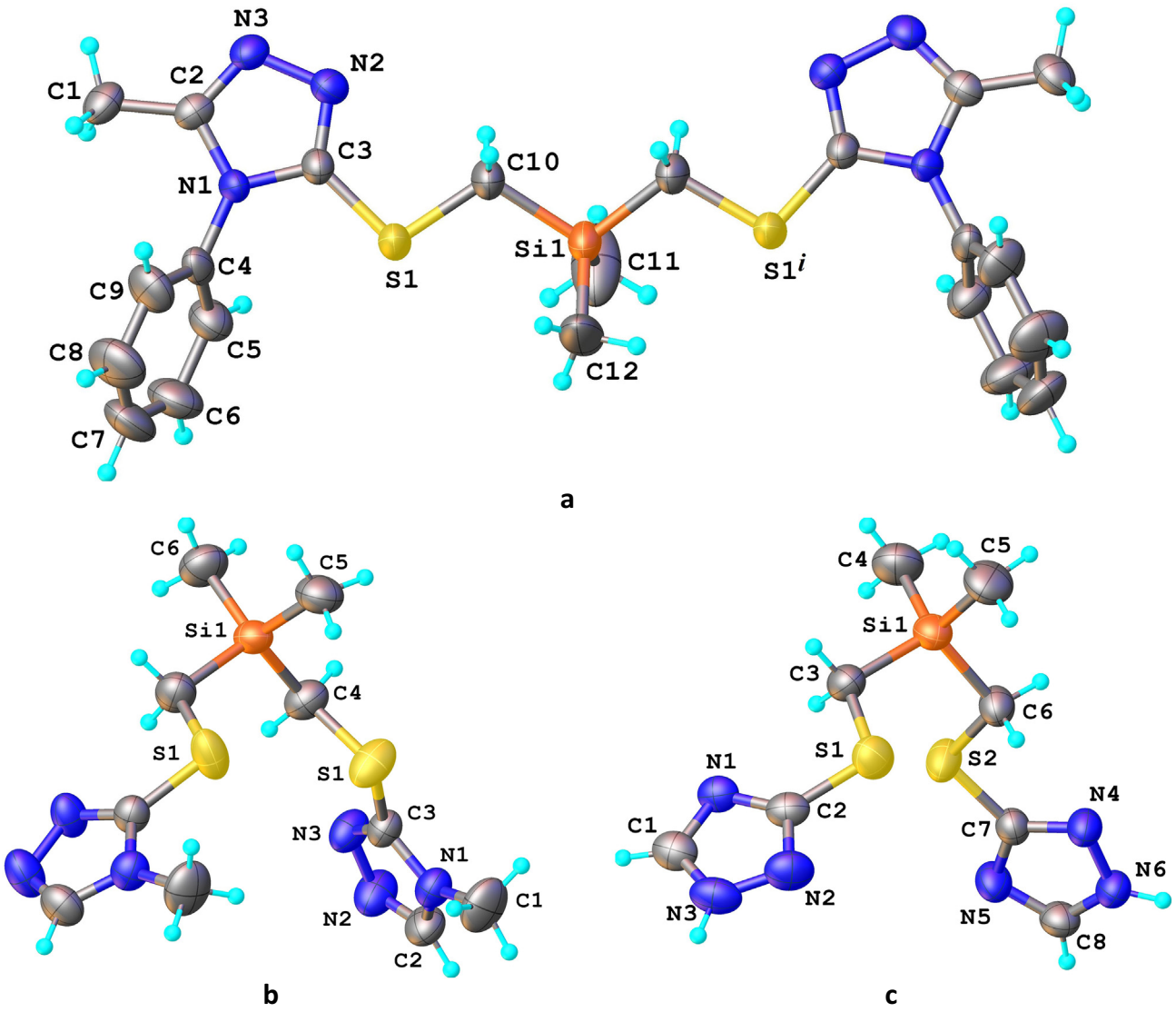

Fig. 5. X-ray molecular structure for: a - compound **5**; b - compound **6**; c – compound **7**, with atom labeling and thermal ellipsoids at 50% probability. Symmetry code *i*) 1 – *x*, *y*, *z*.

groups as donors and nitrogen atoms as acceptors from two distinct triazole rings (Fig. 7).

3.2. Assessment of metal bonding capacity

3.2.1. UV–vis titration

In a recent study, 1,3-bis[5-(2-hydroxyphenyl)-4-phenyl-1,2,4-triazole-3-yl-thio]propane has been shown to act as a fluorescence sensor for the detection of Zn^{2+}, Cu^{2+} and Ni^{2+} [56]. The ability to form complexes with transition metal ions and potentially act as sensors was also investigated for our compounds. According to the Irving-Wiliam's [57], the divalent 3d metals are placed in the following order after the stability constant: Mn < Co < Ni<Cu>Zn, which has been confirmed for a great variety of ligands. For evaluation of sensing properties of bis-triazole **2**–**7** we considered Mn^{2+} ion, the last in the series, and Cu^{2+} and Zn^{2+}, the first in the Irving-William's order. The absorption spectra of the triazole derivatives **2**–**7** recorded in methanol solution (Fig. 8) reveal a maximum at 240–257 nm, assigned to the π-π* transitions in the triazole ring. Initially, the cation binding ability was studied by monitoring the changes in the absorption spectra during the titration of triazole derivatives with a solution of $CuCl_2$ in methanol. Addition of different volumes of 0.1 mM $CuCl_2$ solutions (0.05 to 2 mL) red shifted the band assigned to the triazole ring by 12–20 nm. The new band has been assigned to the LMCT (dπ(Cu(II)) → π*(L)), confirming the coordination of Cu^{2+} ion by the triazole ring.

Under the same conditions, the sensing properties of bis-triazoles **2**–**7** were also tested towards Zn^{2+} and Mn^{2+} but no change in the absorption maximum or the appearance of a novel band was noticed after sequential addition of increasing volumes of solutions containing either Zn^{2+} or Mn^{2+} to the solution of bis-triazoles. Therefore, bis-triazoles **2**–**7** demonstrate a high selectivity towards Cu^{2+} in methanolic solution. A similar tendency of Cu(II) and Zn(II) towards different ligands has been noted previously, when Cu^{2+} was strongly complexed by organic ligands, while a substantial part of Zn^{2+} remained as free Zn^{2+} in the water of an eutrophic lake [58]. This is not surprising, since Cu^{2+} binds to most ligands at least 100 times stronger than Zn^{2+} does [59]. With many ligands, copper(II) complexes are more stable than their zinc(II) counterparts, but increasing ligand rigidity has been shown to improve selectivity towards Zn(II) [60]. The structural flexibility of our triazole derivatives could explain the selectivity for Cu(II) complex formation. Addition of Cu^{2+} changed the color of the solution from colorless to greenish due to the formation of the Cu(II) complex, while the addition of Zn^{2+} or Mn^{2+} to the triazole solution did not cause any change in color. The color and the stability of the Cu(II) complex in solution was monitored in time, and there was no change in the absorption maxima or the color of the solution after one week.

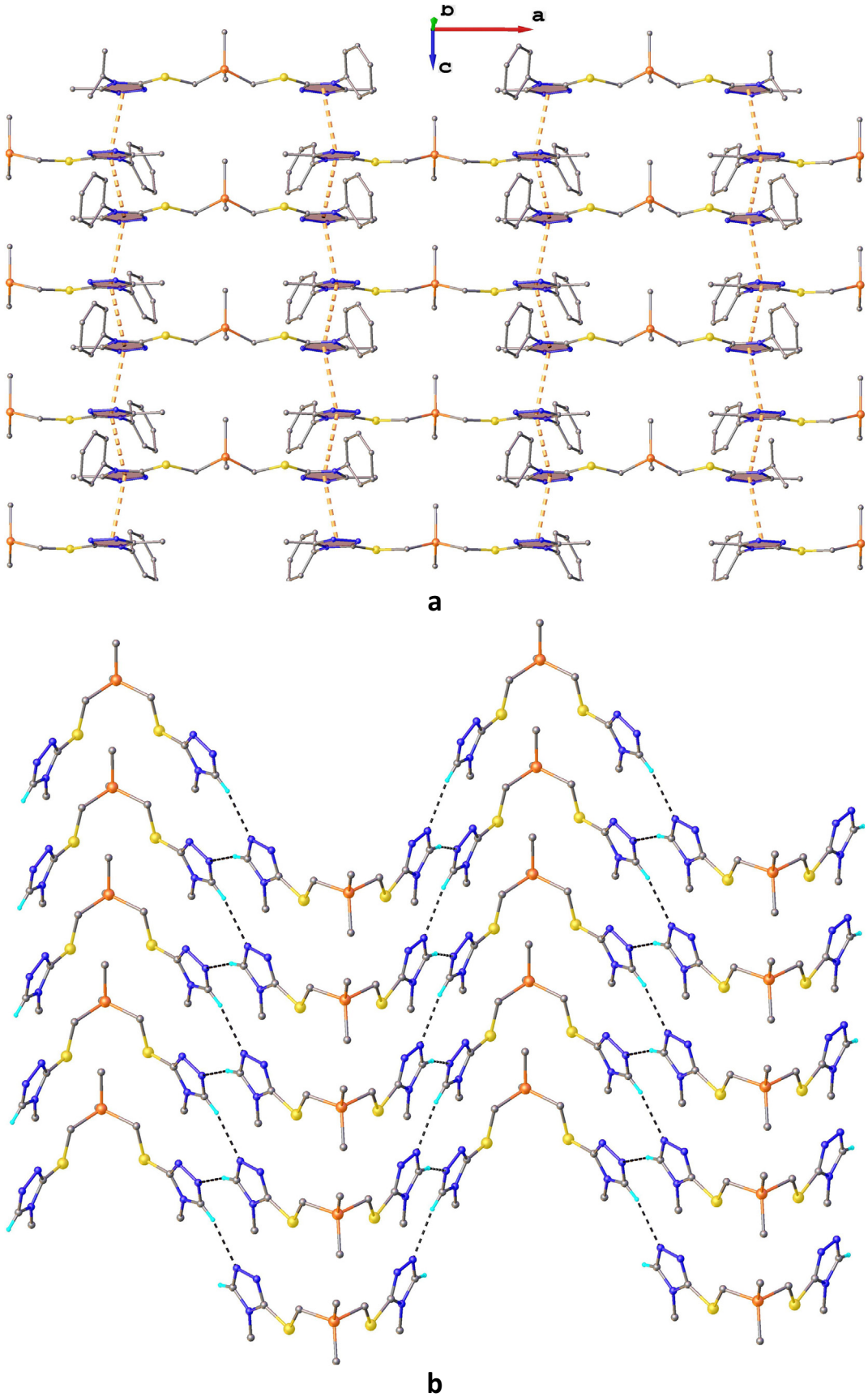

Fig. 6. View of two-dimensional supramolecular architecture in the crystal structure **5** (a) and **6** (b). Centroid-to-centroid distances and H-bonds are drawn in dashed orange and black lines, respectively. Non-relevant H-atoms are not shown. H-bond parameters: C2-H—N2 [C2—H 0.93 Å, H—N2 2.501 Å, C2-H—N2(1.5 – *x*, *y* – 0.5, 1 – *x*) 3.406(3) Å, ∠C2HN2 164.4°].

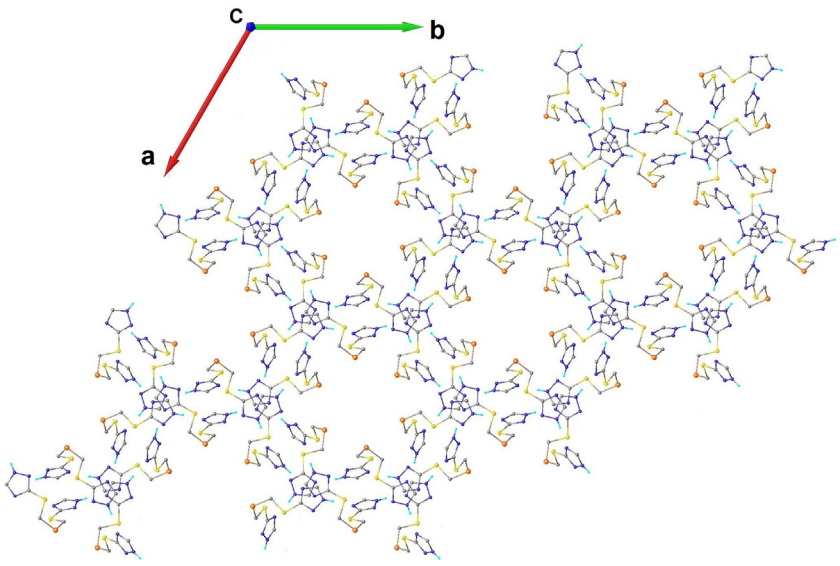

Fig. 7. Crystal structure packing of compound **7**, viewed along *c* crystallographic axis. The methyl groups of the silane fragments are not shown for clarity. H-bonds parameters: N3-H—N5 [N3—H 0.86 Å, H—N5 1.98 Å, N3—N5(5/3 - *y*, 1/3 + x - *y*, *z* – 2/3) 2.835(3) Å, ∠N3HN5 173.0°]; N6-H—N1 [N6—H 0.86 Å, H—N1 1.93 Å, N6—N1(1/3 + *y*, 2/3 –*x* + *y*, 2/3 – *z*) 2.815(4) Å, ∠N3HN1 172.5°].

The binding energies were computed taking into account the coordination possibility of compound **7** (as a ligand **L(7)**) to metal ions studied experimentally (Cu^{2+}, Zn^{2+}, Mn^{2+}) and two other metals (Co^{2+}, Ni^{2+}) in the Irving-Wiliam's series [57]. The theoretical results predict that the complexation of Cu(II) (see Table 2) is more favored, which is consistent with experimental results.

3.2.2. Stoichiometry

From the UV–vis titration experiments, the stoichiometric ratio of each triazole derivatives to Cu^{2+} and the binding constant of the complex (K) were calculated. The [Cu^{2+}]/[L] ratios were 4.69 (**2**), 4.37 (**3**), 5.5 (**4**), 4.8 (**5**), 5.0 (**6**) and 4.9 (**7**) when the plots of the absorbance at 248 nm (**2**), 249 nm (**3**), 240 nm (**4**), 257 nm (**5**), 250 nm (**6**), 243 nm (**7**) were extrapolated, which indicate a 1:1 (L:M) stoichiometry for all the complexes (Fig. 9).

The stoichiometry was also determined by Job's method [61] in the case of compound **2**. In this study, the total concentration (2.5×10^{-5} M) of the triazole derivatives and metal ion was kept constant, while the molar ratio metal ion/ligand was changed from 0 to 1. The Job's plot data are shown in Table S2.

The plotted data (Fig. S25) show that the absorbance of the complex reached a maximum when the molar ratio between Cu^{2+} and triazole derivative **2** is approximately 0.5, which is indicative of a 1:1 complex formation.

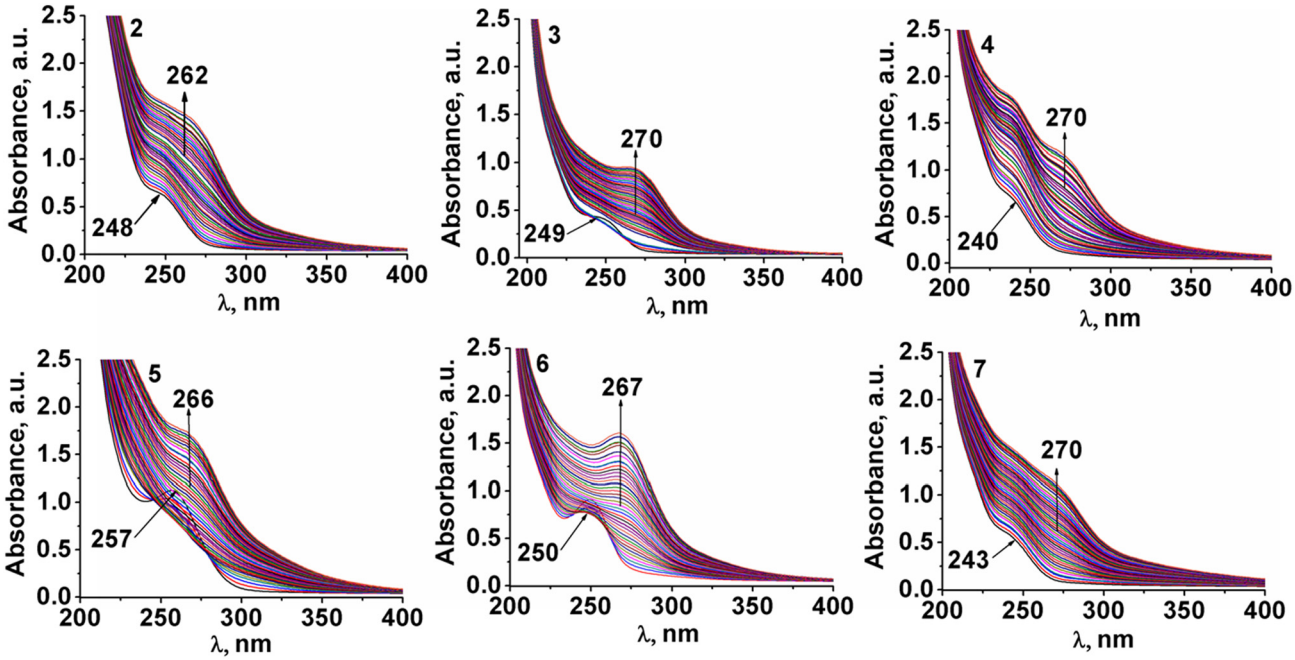

Fig. 8. Changes in the UV–vis spectra of triazole derivatives **2**–**7** during titration with a solution of $CuCl_2$. [Cu^{2+}] mol/L: 1.75×10^{-6}, 3.5×10^{-6}, 5.4×10^{-6}, 7.5×10^{-6}, 9.6×10^{-6}, 1.1×10^{-5}, 1.36×10^{-5}, 1.56×10^{-5}, 1.74×10^{-5}, 1.9×10^{-5}, 2.1×10^{-5}, 2.24×10^{-5}, 2.58×10^{-5}, 2.74×10^{-5}, 2.89×10^{-5}, 3.06×10^{-5}, 3.25×10^{-5}, 3.4×10^{-5}, 3.61×10^{-5}, 3.79×10^{-5}, 4.13×10^{-5}, 4.3×10^{-5}, 4.51×10^{-5}, 4.68×10^{-5}, 4.86×10^{-5}, 5.04×10^{-5}, 5.22×10^{-5}, 5.39×10^{-5}, 5.54×10^{-5}, 5.71×10^{-5}, 5.89×10^{-5}, 5.96×10^{-5}, 1.1×10^{-5}, 6.27×10^{-5}, 6.33×10^{-5}, 6.63×10^{-5}, 6.8×10^{-5}, 7.5×10^{-5}, 8.2×10^{-5}, 9.5×10^{-5}, 1.04×10^{-4}.

Table 2
Binding energies of M-L complexes for compound **7** as ligand, **L**(**7**).

Complex	E_{bind} (kcal/mol)
$Cu^{2+}L(7)$	0
$Zn^{2+}L(7)$	287.87
$Mn^{2+}L(7)$	128.74
$Co^{2+}L(7)$	54.85
$Ni^{2+}L(7)$	261.60

3.2.3. Copper binding constant determination

Owing to the great biological and environmental importance, a large number of ligands for recognition and sensing of metal ions has been designed and synthesized. Ligands containing triazole rings have attracted tremendous interest as versatile ligands with a variety of coordination modes to transition metal centers because of the versatile chemistry and the various donor sites of triazoles.

The binding ability of the synthesized bis-triazoles to Cu^{2+} was investigated by determining the binding constant using the Benesi-Hildebrand equation [62]:

$$\frac{[L]}{\Delta A} = \left(\frac{1}{\varepsilon k}\right) + \left(\frac{1}{Ks[M]\varepsilon k}\right)$$

where [L], [M] and ε_k are the concentrations of the ligand (triazole derivative), concentrations of Cu^{2+} and molar absorption coefficient, respectively;

$\Delta A = A - A_0$, [A] is the absorbance at each molar ratio of Cu^{2+} to ligand, and A_0 is the absorbance in the absence of Cu^{2+}.

By plotting $1/\Delta A$ as a function of the $1/[Cu^{2+}]$, where $[Cu^{2+}]$ is the concentration of copper(II) salt, one gets a straight line, whose slope represents the stability constant of the complex (Fig. S26). The values for the binding stability determined by this approach for the six bis-triazoles are presented in Table 3.

The highest value of the binding constant ($8.87 \times 10^3\ M^{-1}$) was obtained for the complex formation between triazole derivative **2** and Cu^{2+}. According to data showed in Table 3, it seems that the presence of the phenyl and methyl moieties as electron donating groups in the triazole ring (compounds **2**, **3**, **5** and **6**) has a positive effect on the complexing properties of the ligands. It can also be observed that, systematically, the values for the siloxane derivatives are slightly higher than those of the silane counterparts. The greater conformational flexibility of the former could be an explanation for this.

3.3. Assessment of antimicrobial activity

Triazole derivatives are often used in anti-infectious therapies, with triazole-based fluconazole being the first-choice antifungal agent, due to its excellent safety, favorable pharmacokinetic characteristics and a broad spectrum of biological activity. A large number of other triazole antifungals are used clinically: voriconazole, itraconazole and posaconazole. Due to lower electron density, the triazole has a lower coordination capacity and therefore lower toxicity, as compared with imidazole isostere [39].

The newly synthesized here bis-triazole compounds containing differently substituted 1,2,4-triazole rings bridged through 1,3-bis(methylene)tetramethyldisiloxane or bis(chloromethyl)dimethylsilane moieties have been evaluated as antibacterials and antifungals using *in vitro* testing against pure cultures of five fungi species (*Aspergillus niger*, *Penicillium frequentans*, *Penicillium fumigatus*, *Alternaria alternate*, *Fusarium*) and against selected Gram-negative (*Pseudomonas aeruginosa*) and Gram-positive (*Bacillus polymyxa*) bacteria. The

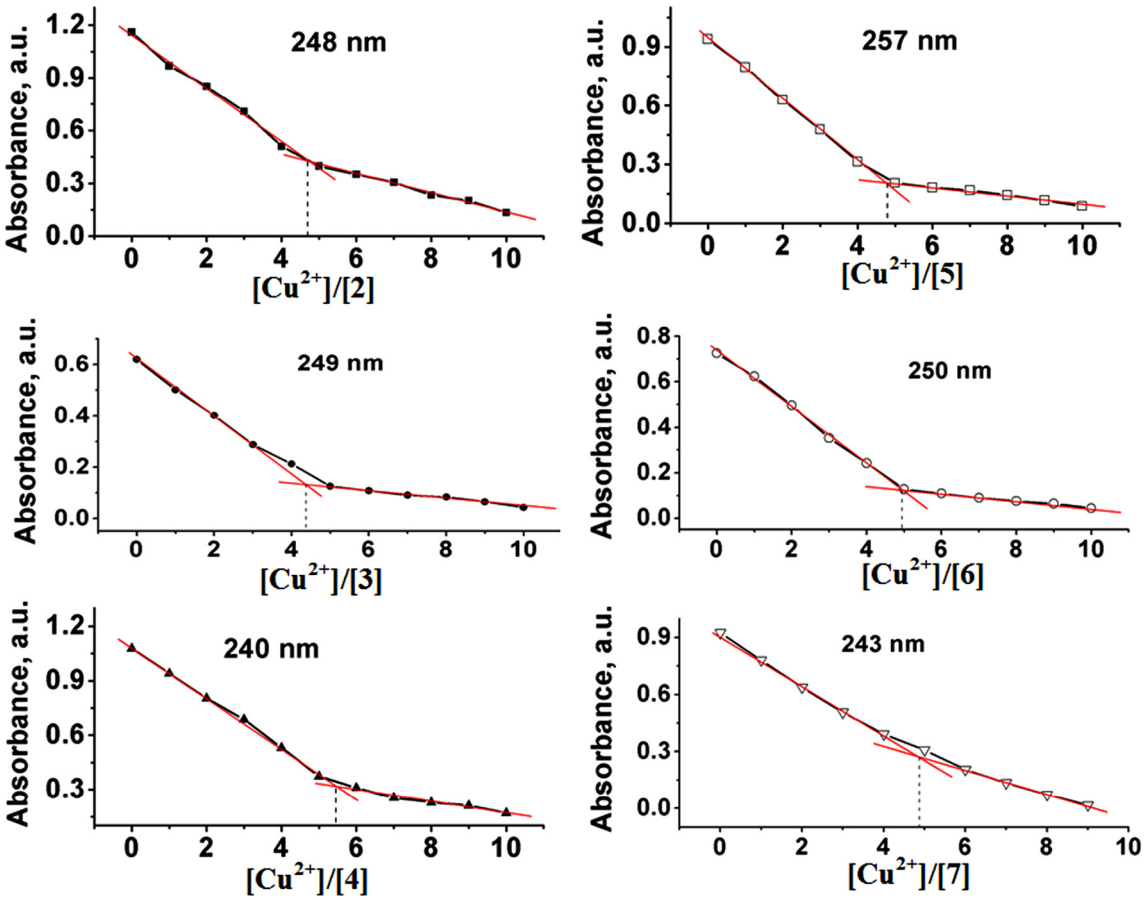

Fig. 9. Plots of the UV–vis absorbance of triazole derivatives **2**–**7** as a function of Cu^{2+} concentration.

Table 3
Binding constant, K, for 1:1 complex formation of the triazole derivative with Cu^{2+} in methanol solution at 25 °C.

Compound	**2**	**3**	**4**	**5**	**6**	**7**
$K \times 10^{-3}$ (M^{-1})	8.87	8.73	7.72	8.56	8.39	7.66

minimum inhibitory concentration (MIC) values obtained for compounds **2**–**7** are summarized in Table S3, and the results are suggestively presented in a concise graphic form in Fig. 10a,b.

The analysis of the results in Table S3 shows that none of the starting materials used in the synthesis of compounds **2**–**7** exhibit significant antimicrobial activity. However, some of the investigated bis-triazoles **2**–**7** are very potent antimicrobial candidates, and their activity is comparable or even higher than that of reference compounds caspofungin and kanamicin. The cause of this manifestation could be one or all of these elements: the presence of two triazole cycles in a single molecule, their coupling by the flexible, highly hydrophobic tetramethyldisiloxane spacer and the presence of thioether bridges. The antimicrobial activity of these compounds becomes more potent

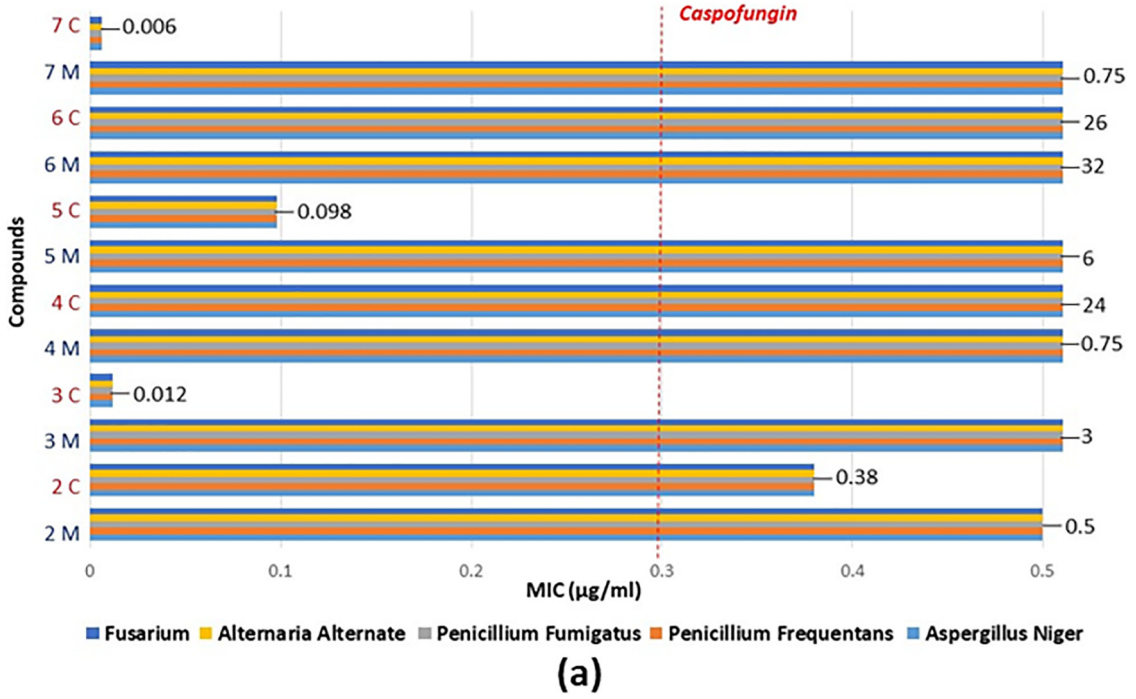

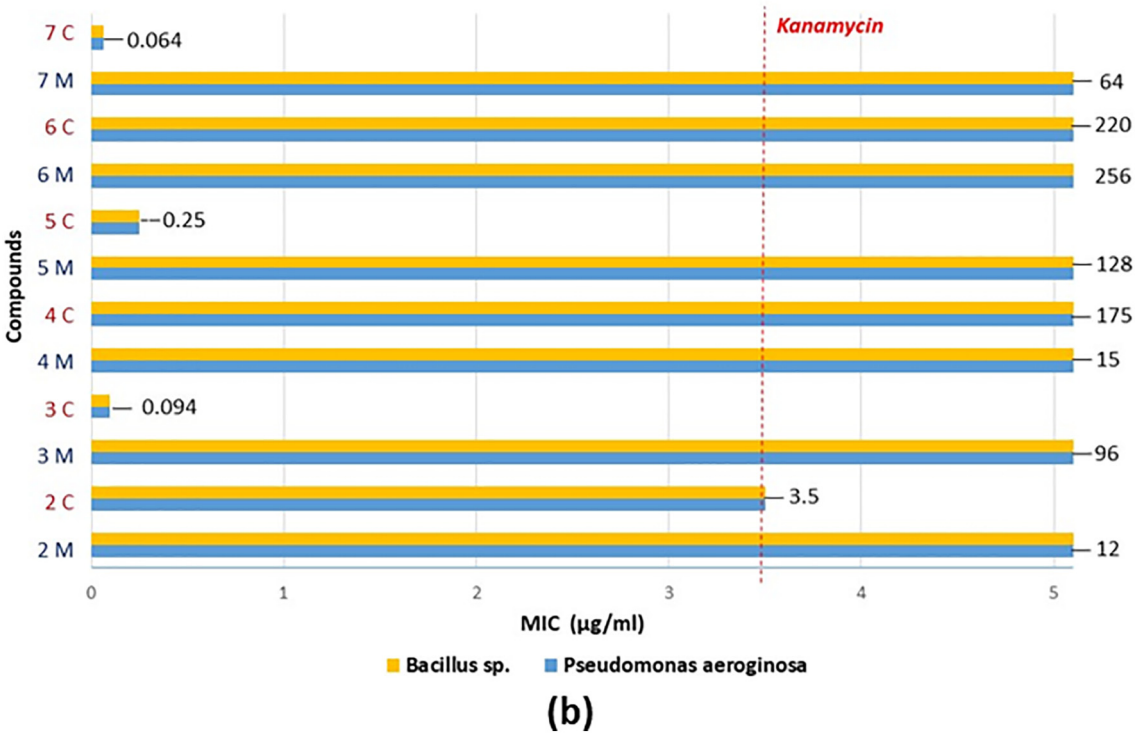

Fig. 10. Comparative representation of antifungal (a) and antibacterial (b) activities (as MIC values) of bis-triazoles **2**–**7** as 1.5 wt% solutions in methanol (M) and chloroform (C).

with the increasing concentration of the sample, and is definitely dependent on the nature of the solvent in which the tested compound is dissolved. Thus, the results obtained for samples of a particular compound dissolved in chloroform are consistently better than the results obtained for the same compound in methanol. Blank tests have shown that chloroform itself exerts a higher antimicrobial activity than methanol. However, the higher activity found for some of the compounds in the bis-triazoles series **2**–**7** in chloroform can not only be attributed to chloroform's own antimicrobial activity. The best biological activity in the series of tested compounds has been recorded for compound **7** at a concentration of 1.5 wt% in chloroform, when this compound was more active than the reference compounds. The MIC values for this compound are 0.006 μg/mL for all fungi, compared to 0.3 μg/mL for caspofungin. Meanwhile, the MIC values are 0.064 μg/mL for both bacterium species, compared to 3.5 μg/mL for reference kanamycin. In contrast, the antimicrobial activity of compound **7** in methanolic solutions is significantly lower, with MIC values of 0.75 μg/mL for fungi and 64 μg/mL for bacteria. Evaluation of compounds **3** and **5** also provided good results against bacteria (MIC values of 0.094 and 0.25 μg/mL, respectively) and fungi (MIC values of 0.098 and 0.012 μg/mL, respectively) when used as a 1.5 wt% solution in chloroform. Compound **2** shows an antimicrobial activity that is similar or comparable to that of the reference drugs.

Previous studies conducted with sixteen 3-mercapto-1,2,4-triazole derivatives support the hypothesis of a correlation between dipole moment values and antibacterial activity [63]. Therefore, the values of the dipole moment have been calculated for compounds **2**–**7** with HF/Lan2DZ and the obtained values are graphically represented in Fig. 11. As can be seen, in **2**–**4** compounds series with siloxane spacers, the dipole moment increases from the 3-mercapto-4-phenyl-5-methyl-1,2,4-triazole derivative to the 3-mercapto-4-methyl-1,2,4-triazole and 3-mercapto-1,2,4-triazole. In contrast, in the silane series, this hierarchy is disturbed by compound **6** derived from 3-mercapto-4-methyl-1,2,4-triazole, which has a dipole moment somewhat higher than compound **7**, which is derived from to 3-mercapto-1,2,4-triazole. As a result, these values alone cannot explain the highest antibacterial activity of compound **7**, for example. Conformational factors may be responsible for this.

In a different study, the structure-activity relationship analysis and computational studies suggested that the most active compounds are those having low lipophilicity and high intrinsic solubility [64]. Compounds **2**–**7** accommodate in their structure the slightly polar and hydrophilic triazole moiety and the highly hydrophobic tetramethyldisiloxane or dimethylsilane segment, linked through a thioether function. The co-existence in a structure of both hydrophilic and hydrophobic fragments is characteristic for surfactants. Because our compounds can be assimilated to surfactants, the hydrophilic-lyophilic balance (HLB) was calculated using the Griffin [65,66] and Davies [67] formula:

$$\mathrm{HLB} = (\%\text{by weight hydrophilic part})/5$$

The obtained HLB values shown graphically in Fig. 11 lie between 3.73 and 7.06, which are characteristic for hydrophobic compounds that include insoluble in water to water-dispersible materials. The HLB values are in an increasing order in each of the two series based on siloxane (**2** < **3** < **4**) and silane (**5** < **6** < **7**) spacer. Compound **7**, which is the most potent candidate in our library, has the highest HLB value (7.06), a correlation that is consistent with the behavior reported in ref. [65]. For the other active compounds, namely **3**, **5** and **2**, the antibacterial activity decreases with decreasing the HLB values. Nevertheless, the biologically poorly active or inactive compounds **4** and **6** also have high HLB values (5.60 and 6.43, respectively), but this lack of activity could be tentatively associated with the influence of the substituents (implicitly their steric effect) from the triazole ring. None of our compounds exhibited a significant antimicrobial activity in methanol, whereas they were very potent when the samples for biological evaluation were prepared in chloroform. This would indicate that solvent-directed conformation and self-assembly factors are responsible for the observed biological activity. A tentative explanation for this behavior could be provided by the results of DLS (Fig. S27) which, in case of methanol solutions, reveals mostly the existence of molecular species having sub-nanometric hydrodynamic diameter values, while in the chloroform, the compounds exist mostly as aggregates of hundreds of nanometers. Understandably, the aggregates in chloroform would be organized with the non-polar tetramethyldisiloxane moiety on the outside, in close contact with the solvent. This arrangement imparts an even more hydrophobic character to these aggregates, and a higher availability for adsorption onto the outer surface of bacteria, in a manner similar to that of alkylimidazolium and alkylpyridinium compounds [68]. It is already accepted that more lipophilic entities can more easily penetrate the cell membrane due to their interaction with fatty acid fragments of the lipid bilayer [64]. It could also be hypothesized that the poor interaction of triazole tails with low polarity solvents allows them to be readily available to interact with the microorganisms (*e.g.*, to coordinate with the heme iron in CYP51), thus inhibiting their growth [69]. The MIC values obtained for the biocidal activity of the compounds described in this paper are better than those reported for triazoles with a more complex structure

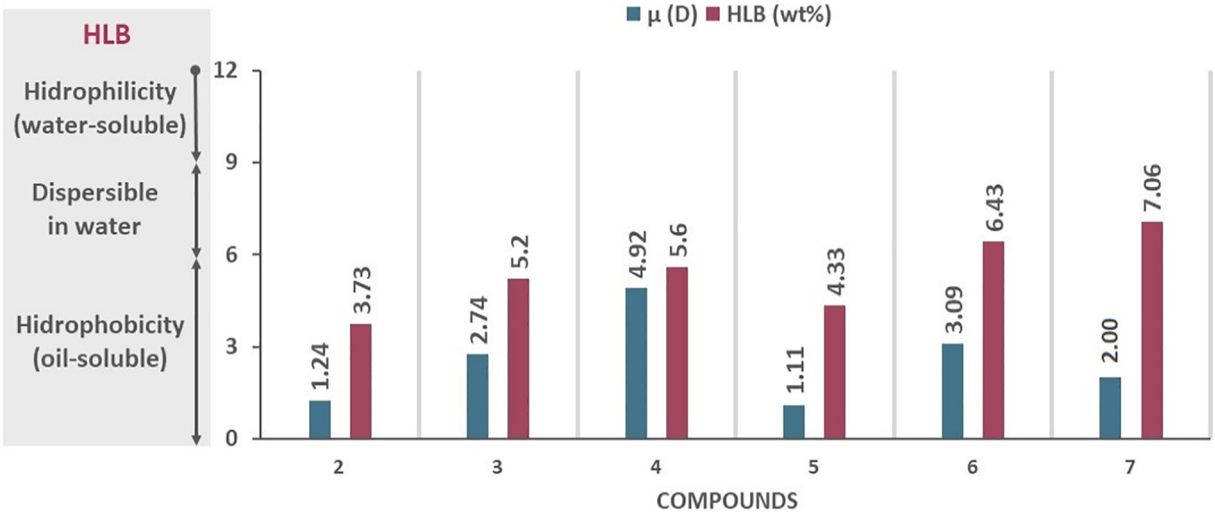

Fig. 11. Comparative graphical representation of the dipole moment (μ) values calculated using HF/Lan2DZ level of theory and the hydrophilic-lyophilic balance (HLB) of compounds **2**–**7**.

[38,70,71]. Another advantage presented by our compounds is that the siloxane bridge is not a risk factor for drug administration and metabolism [72]. It is well-known that silicones are found in many pharmaceutical formulations, generally called Dimethicone or Simethicone, for which no mutagenic, irritating, or acutely toxic effects have been disclosed so far [73].

3.3.1. Molecular docking

Molecular docking calculations were run to predict the inhibitory efficiency of our compounds and to identify the atomic scale interactions responsible for binding. Sterol 14α-Demethylase from *Aspergillus fumigatus* was selected as a possible biologic effector, which could be inhibited by the compounds presented in this study. This is a crucial enzyme for fungal survival, being involved in ergosterol biosynthesis, an important fungal cell membrane component. Therefore, this particular enzyme has become a therapeutic target for many azole-containing anti-fungal agents [74]. The results of theoretical computations based on molecular docking are reflected in Fig. 12.

In silico results show both hydrophobic and hydrophilic interactions between ligands and receptor, as well as π-π stacking interactions in the stabilization of docking complexes, but the hydrophobic interactions are predominant. Interestingly, all docked complexes show the triazole-based ligands directly coordinating the heme ferric iron (residue 601A) with nitrogen atom, where Fe atom plays the role as acceptor

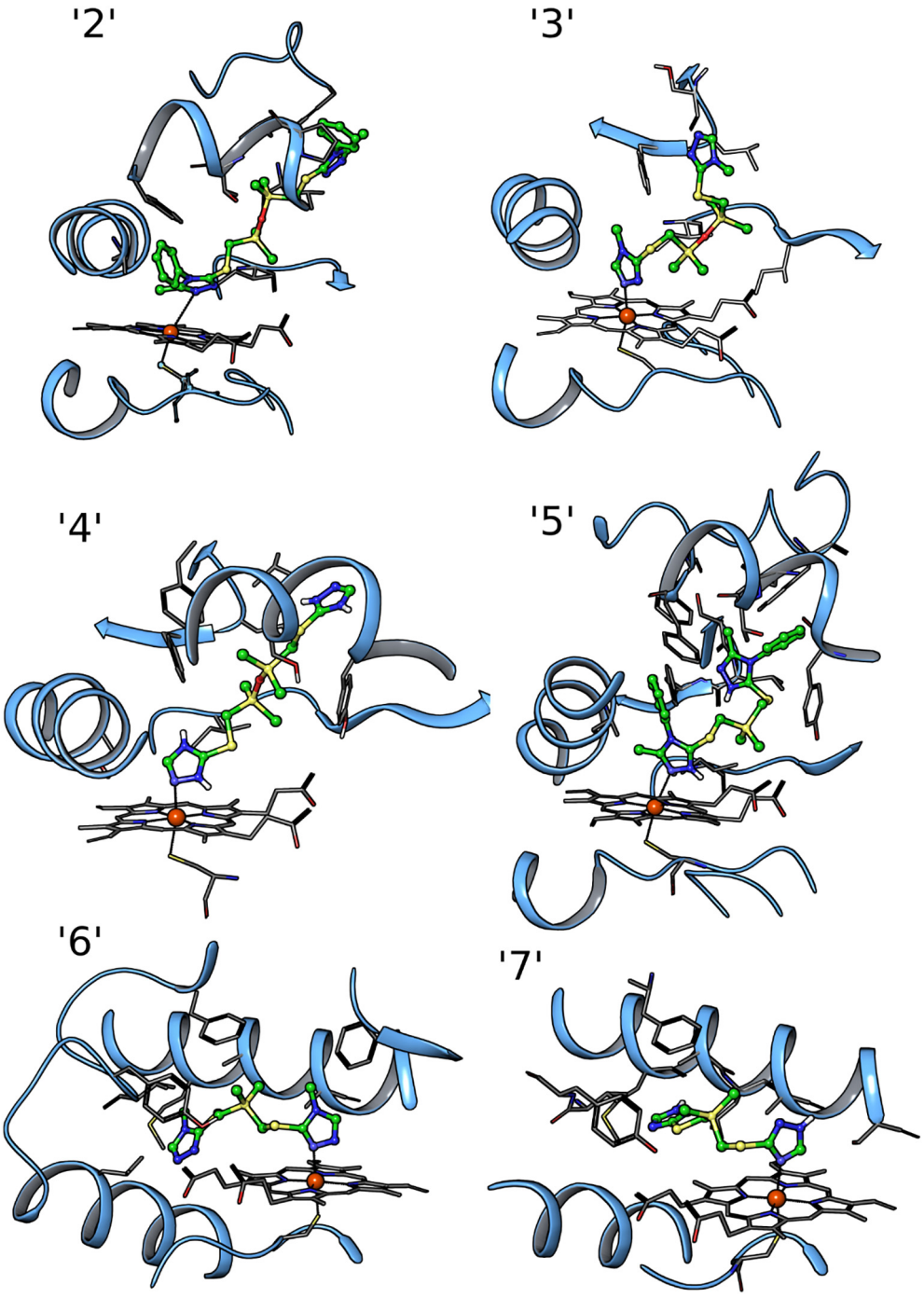

Fig. 12. Molecular representation of the best binding modes for the six studied compounds as resulted from the docking calculations (ball and stick models). Secondary structure elements lining the 14α-Demethylase (CYP51) active sites are represented as ribbons. The heme group and residues important for binding are depicted as sticks. Iron was represented as an orange sphere.

Table 4
Calculated dissociation constants (K_d) for the complexes of the six triazoles-based ligands with the active site of 14α-Demethylase (CYP51) enzyme.

Compound	K_d (μM)
2	4.58×10^{-4}
3	0.428
4	2.52
5	5.14×10^{-3}
6	2.98
7	10.35

of electrons and nitrogen as a donor of electrons. This is in line with the current view, supported by both structural [75–77] and spectroscopic studies [78,79], on the mechanism of action of azole fungicides. The calculated binding affinities, expressed as K_d constants, are presented in Table 4 and these are in the same range as experimentally measured K_ds for medical azoles [80].

4. Conclusions

Reaction of 1,3-bis(chloromethyl)tetramethyldisiloxane and bis (chloromethyl)dimethylsilane with 3-mercapto-1,2,4-triazole derivatives afforded the corresponding bis-triazoles in which the triazole rings are linked to the silicone spacer by thioether bridges. Good yields of crystalline reaction products were obtained, and the structures for five out of six bis-triazoles could be determined by single-crystal X-ray diffraction. All of the novel compounds have a molecular crystal structure, which consists of neutral molecules without any co-crystallized solvent molecules except the compound **5**, which crystalizes with DMF and H_2O molecules in 1:0.5:1 ratio. Due to the high flexibility of the spacer, the compounds with a siloxane bridge can adopt either *trans* or *cis* conformations, while the silane derivatives have a tetrahedral geometry. The average Si—O distance and Si-O-Si angles are of 1.626–1.624 Å and 152.5–155.7°, respectively. The crystal packing of the bis-triazoles is dissimilar and depends on the nature of the substituents from the triazole rings and the type of silicone spacer between them, ranging from discrete, weakly interacting molecules to one-dimensional supramolecular chains, or two-dimensional supramolecular networks (either 2D layers or wave-like 2D network) or a three-dimensional supramolecular motif. All of the triazole derivatives reported in this study preferentially form stable mononuclear 1:1 complexes with Cu(II) in solution, thus suggesting that they could act as chemosensors for Cu detection. The association of triazoles with a silicone component in the same molecule appears to be a promising way to significantly enhance the already well-known biological activity of the triazoles, and to confer a certain degree of selectivity especially in correlation with the polarity of the medium. Theoretical calculations support the obtained experimental results concerning metal binding capacity and biological activity indicating coordination of the heme ferric ion in the particular case of the 14α-Demethylase chosen as a therapeutic target.

Acknowledgement

This work was supported by grants of Ministry of Research and Innovation, CNCS - UEFISCDI, project number PN-III-P4-ID-PCE-2016-0642, within PNCDI III (Contract 114/2017) and project number PN-III-P4-ID-PCCF-2016-0050, within PNCDI III (Contract 4/2018). Grateful thanks to Dr. Cristian-Dragos Varganici for recording the DSC curves and visual designer Andrei Petrariu for graphical abstract.

Appendix A. Supplementary data

Additional figures illustrating NMR spectral data, comments on IR data, crystallographic data, tables containing bond distances (Å) and angles (°), Job's data and plot for compound **2**, data plotting for copper complex stability constant determination of the compound **2**, DLS measurement results, antimicrobial activity tests results, copper complex stability data. Supplementary data to this article can be found online at https://doi.org/10.1016/j.molliq.2019.111560.

References

[1] Missaghi, M.N. Multifunctional Oligomeric Siloxanes: Synthesis and Application to Palladium(II) Oxidation Catalysis. Northwestern University 2010, 3433650.
[2] N. Anbu, A. Dhakshinamoorthy, Cu 3 (BTC) 2 catalyzed dehydrogenative coupling of dimethylphenylsilane with phenol and homocoupling of dimethylphenylsilane to disiloxane, J. Colloid Interf. Sci. 490 (2017) 430–435, https://doi.org/10.1016/j.jcis.2016.11.081.
[3] E. Pouget, J. Tonnar, P. Lucas, P. Lacroix-Desmazes, F. Ganachaud, B. Boutevin, Well-architectured poly(dimethylsiloxane)-containing copolymers obtained by radical chemistry, Chem. Rev. 110 (3) (2010) 1233–1277, https://doi.org/10.1021/cr8001998.
[4] F. Gonzaga, G. Yu, M.A. Brook, Versatile, efficient derivatization of polysiloxanes via click technology, Chem. Commun. (2009) 1730–1732, https://doi.org/10.1039/B821788B.
[5] C. Racleş, M. Cazacu, Siloxane-containing liquid crystalline polymers, Advances in Functional Heterochain Polymers, Nova Science Publishers, ISBN: 978-1-60456-599-7, 2008.
[6] C. Racles, T. Hamaide, Synthesis and characterization of water soluble saccharide functionalized polysiloxanes and their use as polymer surfactants for the stabilization of polycaprolactone nanoparticles, Macromol. Chem. Phys. 206 (2005) 1757–1768, https://doi.org/10.1002/macp.200500139.
[7] C. Racles, Siloxane-based surfactants containing tromethamol units, Soft Mater 8 (3) (2010) 1–11, https://doi.org/10.1080/1539445X.2010.495627.
[8] C. Racles, V. Cozan, Synthesis of glucose-modified siloxanes by a simplified procedure, Soft Mater. 10 (4) (2012) 413–425, https://doi.org/10.1080/1539445X.2010.523752.
[9] A. Vlad, C. Turta, M. Cazacu, E. Rusu, S. Shova, A new bis(pyrrole) Schiff base containing flexible siloxane sequence and its Ni(II) complex, Eur. J. Inorg. Chem. 31 (2012) 5078–5084, https://doi.org/10.1002/ejic.201200612.
[10] A. Soroceanu, M. Cazacu, S. Shova, C. Turta, J. Kožišek, M. Gall, M. Breza, P. Rapta, T.C.O. Mac Leod, A.J.L. Pombeiro, J. Telser, A.A. Dobrov, V.B. Arion, Copper(II) complexes with Schiff bases containing a disiloxane unit: synthesis, structure, bonding features and catalytic activity for benzyl alcohol aerobic oxidation, Eur. J. Inorg. Chem. (2013) 1458–1474, https://doi.org/10.1002/ejic.201201080.
[11] M.-F. Zaltariov, M. Cazacu, N. Vornicu, S. Shova, C. Racles, M. Balan, C. Turta, A new diamine containing disiloxane moiety and some derived Schiff bases: synthesis, molecular and supramolecular structures, and biocidal activity, Supramol. Chem. 25 (8) (2013) 490–502, https://doi.org/10.1080/10610278.2013.794947.
[12] M. Alexandru, M. Cazacu, A. Arvinte, S. Shova, C. Turta, B.C. Simionescu, A. Dobrov, E.C.B.A. Alegria, L.M.D.R.S. Martins, A.J.L. Pombeiro, V.B. Arion, μ-Chlorido-bridged dimanganese(II) complexes of the Schiff base derived from condensation of 2,6-diformyl-4-methylphenol and 1,3-bis(3-aminopropyl)tetramethyldisiloxane: structure, magnetism, electrochemical behaviour and catalytic oxidation of secondary alcohols, Eur. J. Inorg. Chem. 1 (2014) 120–131, https://doi.org/10.1002/ejic.201300969.
[13] A. Vlad, M.-F. Zaltariov, S. Shova, G. Novitchi, C.-D. Varganici, C. Train, M. Cazacu, Flexible linkers and dinuclear metallic nodes build up an original metal-organic framework, CrystEngComm 15 (2013) 5368–5375, https://doi.org/10.1039/C3CE40506K.
[14] M.-F. Zaltariov, A. Vlad, M. Cazacu, S. Shova, M. Balan, C. Racles, Novel siloxane-containing dicarboxylic acid, 1,3-bis(p-carboxyphenylene-ester-methylene) tetramethyldisiloxane, and its derivatives: ester macrocycle and supramolecular structure with a copper complex, Tetrahedron 70 (2014) 2661–2668, https://doi.org/10.1016/j.tet.2014.02.061.
[15] M.-F. Zaltariov, M. Alexandru, M. Cazacu, S. Shova, G. Novitchi, C. Train, A. Dobrov, M.V. Kirillova, E.C.B.A. Alegria, A.J.L. Pombeiro, V.B. Arion, Tetranuclear copper(II) complexes with macrocyclic and open-chain disiloxane containing ligands as catalyst precursors for hydrocarboxylation and oxidation of alkanes and 1-phenylethanol, Eur. J. Inorg. Chem. 29 (2014) 4946–4956, https://doi.org/10.1002/ejic.201402578.
[16] M. Cazacu, S. Shova, A. Soroceanu, P. Machata, L. Bucinsky, M. Breza, P. Rapta, J. Telser, J. Krzystek, V.B. Arion, Charge and spin states in Schiff base metal complexes with a disiloxane unit exhibiting a strong noninnocent ligand character: synthesis, structure, spectroelectrochemistry, and theoretical calculations, Inorg. Chem. 54 (12) (2015) 5691–5706, https://doi.org/10.1021/acs.inorgchem.5b00229.
[17] M.-F. Zaltariov, M. Cazacu, L. Sacarescu, A. Vlad, G. Novitchi, C. Train, S. Shova, V.B. Arion, Oxime-bridged Mn_6 clusters inserted in one-dimensional coordination polymer, Macromolecules 49 (17) (2016) 6163–6172, https://doi.org/10.1021/acs.macromol.6b01149.
[18] S. Shova, M. Cazacu, G. Novitchi, G. Zoppellaro, C. Train, V.B. Arion, An iron(III)-centred ferric wheel Fe subset of{Fe-6} with a siloxane-based bis-salicylidene Schiff base, Dalton Trans. 46 (6) (2017) 1789–1793, https://doi.org/10.1039/C7DT00141J.
[19] S. Shova, A. Vlad, M. Cazacu, J. Krzystek, L. Bucinsky, M. Breza, D. Darvasiova, P. Rapta, J. Cano, J. Telser, V. Arion, A five-coordinate manganese(III) complex of a salen type ligand with a positive axial anisotropy parameter D, Dalton Trans. 46 (35) (2017) 11817–11829, https://doi.org/10.1039/C7DT01809F.

[20] T. Akimoto, Y. Nagase, Novel transdermal drug penetration enhancer: synthesis and enhancing effect of alkyldisiloxane compounds containing glucopyranosyl group, J. Control. Release 88 (2003) 243–252, https://doi.org/10.1016/S0168-3659(03)00006-3.
[21] A. Misra, A. Shahiwala, Applications of Polymers in Drug Delivery, Smithers Rapra, 2014, ISBN 978-1-84735-853-0.
[22] L.G. Shagun, I.A. Dorofeev, L.V. Zhilitskaya, L.I. Larina, N.O. Yarosh, L.V. Klyba, E.R. Sanzheeva, One-pot synthesis of first imidazolophanes with dimethylene (tetramethyl)disiloxane spacers, Mendeleev Commun. 25 (2015) 34–35, https://doi.org/10.1016/j.mencom.2015.01.012.
[23] B. Delord, M.C. Guillorit, J. Lafayz, M.L. Andreola, D. Tharaud, S. Litvak, H. Fleuryl, G. Deleris, Novel C-organosilicon derivatives as leads for reverse-transcriptase-mediated anti-HIV-l activity, Eur. J. Med. Chem. 31 (1996) 111–122, https://doi.org/10.1016/0223-5234(96)80444-2.
[24] F.L.S. Tse, T. Chang, B. Finkelstein, F. Ballard, J.M. Jaffe, Influence of mode of intravenous administration and blood sample collection on rat pharmacokinetic data, J. Pharm. Sci. 73 (1984) 1599–1602, https://doi.org/10.1002/jps.2600731128.
[25] M.J. Ardolino, Development and Application of Disiloxanes as a New Class of Hard Anion-binding Organocatalysts, Harvard University, Cambridge, MA, United States, 2015-2016http://grantome.com/grant/NIH/F32-GM113414-02.
[26] H. Takuda, T. Maoka, N. Suzuiki, J. Nohmann, A. Vasas, H. Engi, I. Mucsi, U. Olszewskis, G. Hamiltons, L. Amaral, J. Molnar, Effects of two disiloxanes ALIS-409 and ALIS-421 on chemoprevention in model experiments, Anticancer Res. 33 (2013) 2021–2028.
[27] Ş.G. Küçükgüzel, P. Çıkla-Süzgün, Recent advances bioactive 1,2,4-triazole-3-thiones, Eur. J. Med. Chem. 97 (2015) 830–870, https://doi.org/10.1016/j.ejmech.2014.11.033.
[28] R. Kharb, P.C. Sharma, M.S. Yar, Pharmacological significance of triazole scaffold, J. Enzyme Inhib. Med. Chem. 26 (1) (2011) 1–21, https://doi.org/10.3109/14756360903524304.
[29] Y. Ünver, S. Deniz, F. Çelik, Z. Akar, M. Küçük, K. Sancak, Synthesis of new 1,2,4-triazole compounds containing Schiff and Mannich bases (morpholine) with antioxidant and antimicrobial activities, J. Enzyme Inhib. Med. Chem. 31 (2016) 89–95, https://doi.org/10.1080/14756366.2016.1206088.
[30] T. Plech, B. Kaproń, A. Paneth, U. Kosikowska, A. Malm, A. Strzelczyk, P. Stączek, Ł. Świątek, B. Rajtar, M. Polz-Dacewicz, Search for factors affecting antibacterial activity and toxicity of 1,2,4-triazole-ciprofloxacin hybrids, Eur. J. Med. Chem. 97 (2015) 94–103, https://doi.org/10.1016/j.ejmech.2015.04.058.
[31] X. Chai, S. Yu, Y. Jiang, Y. Zou, Q. Wu, D. Zhang, Y. Jiang, Y. Cao, Q. Sun, Design, synthesis, and biological evaluation of novel 1, 2, 4-triazole derivatives as antifungal agent, Arch. Pharm. Res. 35 (11) (2012) 1895–1901, https://doi.org/10.1007/s12272-012-1105-8.
[32] R. Kaur, A.R. Dwivedi, B. Kumar, V. Kumar, Recent developments on 1,2,4-triazole nucleus in anticancer compounds: a review, Anti-Cancer Agent. Me. 16 (4) (2016) 465–489, https://doi.org/10.2174/1871520615666150819121106.
[33] M. Abdel-Aziz, E.A. Beshr, I.M. Abdel-Rahman, K. Ozadali, O.U. Tan, O.M. Aly, 1-(4-Methoxyphenyl)-5-(3,4,5-trimethoxyphenyl)-1H-1,2,4-triazole-3-carboxamides: synthesis, molecular modeling, evaluation of their anti-inflammatory activity and ulcerogenicity, Eur. J. Med. Chem. 77 (2014) 155–165, https://doi.org/10.1016/j.ejmech.2014.03.001.
[34] S. Zhang, Z. Xu, C. Gao, Q.C. Ren, L. Chang, Z.S. Lv, L.S. Feng, Triazole derivatives and their anti-tubercular activity, Eur. J. Med. Chem. 138 (2017) 501–513, https://doi.org/10.1016/j.ejmech.2017.06.051.
[35] A. Ayati, S. Emami, A. Foroumadi, The importance of triazole scaffold in the development of anticonvulsant agents, Eur. J. Med. Chem. 109 (2016) 380–392, https://doi.org/10.1016/j.ejmech.2016.01.009.
[36] H.T. Balaydın, M. Özil, M. Şentürk, Synthesis and glutathione reductase inhibitory properties of 5-methyl-2,4-dihydro-3H-1,2,4-triazol-3-one's aryl Schiff base derivatives, Arch. Pharm. (Weinheim) (2018), e1800086. https://doi.org/10.1002/ardp.201800086.
[37] E. Başaran, A. Karaküçük-Iyidoğan, D. Schols, E.E. Oruç-Emre, Synthesis of novel chiral sulfonamide-bearing 1,2,4-triazole-3-thione analogs derived from D- and L-phenylalanine esters as potential anti-influenza agents, Chirality 28 (6) (2016) 495–513, https://doi.org/10.1002/chir.22607.
[38] T. Önkol, D.S. Doğruer, L. Uzun, S. Adak, S. Özkan, M.F. Şahin, Synthesis and antimicrobial activity of new 1,2,4-triazole and 1,3,4-thiadiazole derivatives, J. Enzym Inhib. Med. Ch. 23 (2) (2008) 277–284, https://doi.org/10.1080/14756360701408697.
[39] Y. Zhang, G.L.V. Damu, S. Cui, J. Mi, V.K.R. Tangadanchu, C. Zhou, Discovery of potential antifungal triazoles: design, synthesis, biological evaluation, and preliminary antifungal mechanism exploration, Med Chem Comm. 8 (2017) 1631–1639, https://doi.org/10.1039/C7MD00112F.
[40] A.S. Belapure, Synthesis and Catalytic Applications of 1,2,4-Triazoles in Oxidative Processes, PhD diss. University of Tennessee, 2012.
[41] I. Bräunlich, Polynuclear Metal(II) Complexes With 1,2,4-Triazole Derivatives, ETH ZURICH, 2014https://doi.org/10.3929/ethz-a-010251009 Diss. ETH No. 22187.
[42] M. Vinod, J. Keshavayya, V.P. Vaidya, M.H. Moinuddin Khan, Triazoles as complexing agents: synthesis, characterization and pharmacological activities of copper complexes of 4-amino-3-mercapto-5-substituted aryl-1,2,4-triazoles, J. Coord. Chem. 61 (16) (2008) 2629–2638, https://doi.org/10.1080/00958970801950615.
[43] Y. Mu, G. Han, Z. Li, X. Liu, H. Hou, Y. Fan, Effect of organic polycarboxylate ligands on the structures of a series of zinc(II) coordination polymers based on a conformational bis-triazole ligand, Cryst. Growth Des. 12 (3) (2012) 1193–1200, https://doi.org/10.1021/cg201180u.
[44] L.G. Shagun, I.A. Dorofeev, L.V. Zhilitskaya, N.O. Yarosh, L.I. Larina, Synthesis of the first siloxane derivatives of triazoles, Chem. Heterocyc. Compd. 50 (2014) 1332, https://doi.org/10.1007/s10593-014-1596-y.
[45] M. Kazemi, H. Kohzadi, O. Abdi, Alkylation of thiols in green mediums, J. Mater. Environ. Sci. 6 (5) (2015) 1451–1456.
[46] J. Zhang, L. Weng, X. Su, G. Lu, W. Liu, Y. Tang, Y. Zhang, J. Wen, Z. Teng, L. Wang, Cisplatin and doxorubicin high-loaded nanodrug based on biocompatible thioether- and ethane-bridged hollow mesoporous organosilica nanoparticles, J. Colloid Interf. Sci. 513 (2018) 214–221, https://doi.org/10.1016/j.jcis.2017.10.116.
[47] CrysAlis RED, Oxford Diffraction Ltd., Version 1.171.36.32, 2003.
[48] O.V. Dolomanov, L.J. Bourhis, R.J. Gildea, J.A.K. Howard, H. Puschmann, J. Appl. Crystallogr. 42 (2009) 339–341.
[49] G.M. Sheldrick, SHELXS, Acta Cryst A64 (2008) 112–122.
[50] M.J. Frisch, G.W. Trucks, H.B. Schlegel, G.E. Scuseria, M.A. Robb, J.R. Cheeseman, G. Scalmani, V. Barone, B. Mennucci, H. Petersson, et al., Gaussian 09, Revision B.01, Gaussian, Inc., Wallingford, CT, 2009.
[51] G.M. Morris, R. Huey, W. Lindstrom, M.F. Sanner, R.K. Belew, D.S. Goodsell, A.J. Olson, Autodock4 and AutoDockTools4: automated docking with selective receptor flexiblity, J. Comput. Chem. 16 (2009) 2785–2791.
[52] L. Friggeri, T.Y. Hargrove, Z. Wawrzak, A.L. Blobaum, G. Rachakonda, C.W. Lindsley, F. Villalta, W.D. Nes, M. Botta, F.P. Guengerich, G.I. Lepesheva, Sterol 14α-demethylase structure-based design of VNI ((*R*)-*N*-(1-(2,4-dichlorophenyl)-2-(1*H*-imidazol-1-yl)ethyl)-4-(5-phenyl-1,3,4-oxadiazol-2-yl)benzamide)) derivatives to target fungal infections: synthesis, biological evaluation, and crystallographic analysis, J. Med. Chem. 61 (13) (2018) 5679–5691, https://doi.org/10.1021/acs.jmedchem.8b00641.
[53] S.J. Cavalieri, R.J. Harbeck, Y.S. McCarter, J.H. Ortez, I.D. Rankin, R.L. Sautter, S.E. Sharp, C.A. Spiegel, Manual of antimicrobial susceptibility testing, in: Marie B. Coyle (Ed.), Library of Congress Cataloging-in-publication Data, American Society for Microbiology press, Washington DC. USA 2005, p. 220.
[54] J. Khurana, P.K. Sahoo, Chemoselective alkylation of thiols: a detailed investigation of reactions of thiols with halides, Synth. Commun 22 (12) (1992) 1691–1702, https://doi.org/10.1080/00397919208020489.
[55] X.X. Wu, B. Ding, R.N. Chang, H.A. Zou, Z.Z. Zhu, A new complex of Mn(II) with highly flexible bistriazole ligand 1,2-bis(1,2,4-triazole-l-yl) ethane: synthesis and crystal structure, Russ. J. Coord. Chem. 37 (6) (2011) 431–434, https://doi.org/10.1134/S1070328411050137.
[56] R.E. Sabzi, A. Nikoo, Y. Nikzad, M. Bahram, K. Akbari, N. Samadi, Synthesis and determination of stability constants of a new bis-1,2,4-triazole ligand for complexation with zinc(II), copper(II) and nickel(II) in acetonitrile, Am. J. Analyt. Chem. 3 (2012) 437–442, https://doi.org/10.4236/ajac.2012.36057.
[57] H. Irving, R.J.P. Williams, The stability of transition-metal complexes, J. Chem. Soc. (1953) 3192–3210, https://doi.org/10.1039/jr9530003192.
[58] H.B. Xue, D. Kistler, L. Sigg, Competition of copper and zinc for strong ligands in a eutrophic lake, Limnol. Oceanogr. 40 (6) (1995) 1142–1152, https://doi.org/10.4319/lo.1995.40.6.1142.
[59] J.J.R. Frausto da Silva, R.J.P. Williams, The Biological Chemistry of the Elements: The Inorganic Chemistry of Life, 2nd edition Oxford University Press, 2001 48.
[60] Z. Dai, X. Xu, J.W. Canary, Stereochemical control of Zn(II)/Cu(II) selectivity in piperidine tripod ligands, Chem. Commun. (2002) 1414–1415, https://doi.org/10.1039/B111259G.
[61] P. Job, Formation and stability of inorganic complexes in solution, Ann. Chim. Applicata 9 (1928) 113–203.
[62] H.A. Benesi, J.H. Hildebrand, A spectrophotometric investigation of the interaction of iodine with aromatic hydrocarbons, J. Am. Chem. Soc. 71 (1949) 2703–2707.
[63] T. Plech, M. Wujec, U. Kosikowska, A. Malm, Synthesis and antibacterial activity of 4,5-disubstituted-1,2,4-triazole-3-thiones, Lett. *Drug Des. Discov.* 10 (10) (2013) 917–922, https://doi.org/10.2174/15701808113109990082.
[64] S. Alyar, N. Karacan, Synthesis, characterization, antimicrobial activity and structure–activity relationships of new aryldisulfonamides, J. Enzyme Inhib. Med. Chem. 24 (4) (2009) 986–992, https://doi.org/10.1080/14756360802561220.
[65] W.C. Griffin, Classification of surface-active agents by 'HLB', J. Soc. Cosmet. Chem. 1 (5) (1949) 311–326.
[66] W.C. Griffin, Calculation of HLB values of non-ionic surfactants, J. Soc. Cosmet. Chem. 5 (4) (1954) 249–256.
[67] J.T. Davies, A quantitative kinetic theory of emulsion type, I. physical chemistry of the emulsifying agent. Gas/liquid and liquid/liquid interface, Proceedings of the International Congress of Surface Activity 1957, pp. 426–438.
[68] A. Cornellas, L. Perez, F. Comelles, I. Ribosa, A. Manresa, M.T. Garcia, Self-aggregation and antimicrobial activity of imidazolium and pyridinium based ionic liquids in aqueous solution, J. Colloid Interf. Sci. 355 (2011) 164–171, https://doi.org/10.1016/j.jcis.2010.11.063.
[69] H. Sadeghpour, S. Khabnadideh, K. Zomorodian, K. Pakshir, K. Hoseinpour, N. Javid, E. Faghih-Mirzaei, Z. Rezaei, Design, synthesis, and biological activity of new triazole and nitro-triazole derivatives as antifungal agents, Molecules 22 (7) (2017) 1150, https://doi.org/10.3390/molecules22071150.
[70] V. Sumangala, B. Poojary, N. Chidananda, J. Fernandes, S. Kumari, Synthesis and antimicrobial activity of 1,2,3-triazoles containing quinoline moiety, Arch. Pharm. Res. 33 (12) (2010) 1911–1918, https://doi.org/10.1007/s12272-010-1204-3.
[71] D. Gupta, D.K. Jain, Synthesis, antifungal and antibacterial activity of novel 1,2,4-triazole derivatives, J. Adv. Pharm. Technol. Res. 6 (3) (2015) 141–146, https://doi.org/10.4103/2231-4040.161515.
[72] S. Varaprath, K.L. Salyers, K.P. Plotzke, S. Nanavati, Identification of metabolites of octamethylcyclotetrasiloxane (D_4) in rat urine, Drug Metab. Dispos. 27 (11) (1999) 1267–1273.
[73] A. Colas, J. Siang, K. Ulman, Silicones in Pharmaceutical Applications, Dow Corning Corporation, 2006 52–1090-01.
[74] E. Mellado, L. Alcazar-Fuoli, M. Cuenca-Estrella, J.L. Rodriguez-Tudela, Role of Aspergillus lentulus 14-α Sterol Demethylase (Cyp51A) in Azole Drug Susceptibility,

Antimicrob. Agents Chemother. 12 (12) (2011) 5459–5468, https://doi.org/10.1128/aac.05178-11 (2011).
[75] L.M. Podust, T.L. Poulos, M.R. Waterman, Crystal structure of cytochrome P450 14alpha-sterol demethylase (Cyp51) from Mycobacterium tuberculosis in complex with azole inhibitors, Proc. Natl. Acad. Sci. USA 98 (2001) 3068–3073.
[76] G.I. Lepesheva, T.Y. Hargrove, S. Anderson, Y. Kleshchenko, V. Furtak, Z. Wawrzak, F. Villalta, M.R. Waterman, Structural insights into inhibition of sterol 14{alpha}-demethylase in the human pathogen Trypanosoma cruzi, J. Biol. Chem. 285 (2010) 25582–25590.
[77] A.A. Sagatova, M.V. Keniya, R.K. Wilson, M. Sabherwal, J.D. Tyndall, B.C. Monk, Triazole resistance mediated by mutations of a conserved active site tyrosine in fungal lanosterol 14 alpha-demethylase, Sci. Rep. 6 (2016) 26213.
[78] A.G.S. Warrilow, C.M. Martel, J.E. Parker, N. Melo, D.C. Lamb, W. David Nes, D.E. Kelly, S.L. Kelly, Azole binding properties of *Candida albicans* sterol 14-α demethylase (CaCYP51), Antimicrob. Agents Chemother. 54 (10) (2010) 4235–4245, https://doi.org/10.1128/AAC.00587-10.
[79] A.G.S. Warrilow, C.L. Price, J.E. Parker, N.J. Rolley, C.J. Smyrniotis, D.D. Hughes, V. Thoss3, W.D. Nes, D.E. Kelly, T.R. Holman, S.L. Kelly, Azole antifungal sensitivity of sterol 14α-demethylase (CYP51) and CYP5218 from *Malassezia globose*, Sci. Rep. 6 (2016), 27690. https://doi.org/10.1038/srep27690.
[80] A.G. Warrilow, J.E. Parker, D.E. Kelly, S.L. Kelly, Azole affinity of sterol 14α-demethylase (CYP51) enzymes from *Candida albicans* and *Homo sapiens*, Antimicrob. Agents Chemother. 57 (3) (2013) 1352–1360, https://doi.org/10.1128/AAC.02067-12.